

Results on the production of light (anti)(hyper)nuclei at the LHC

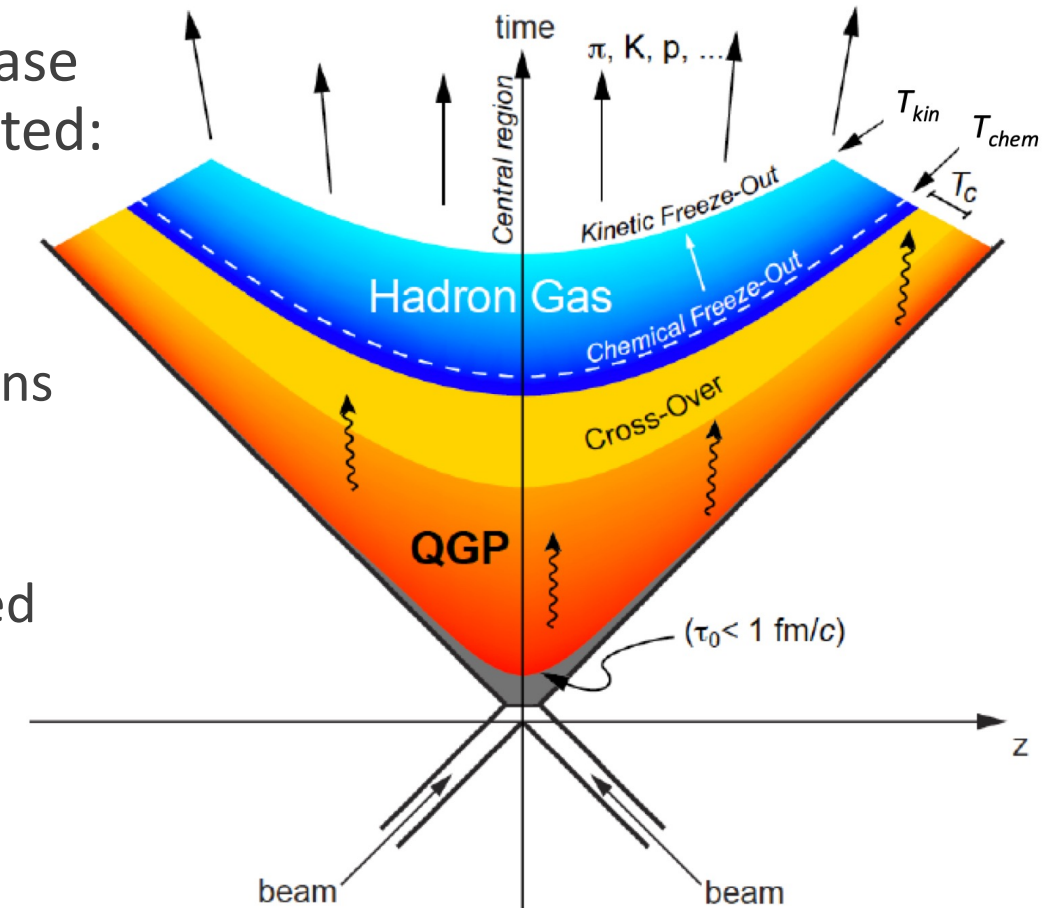
ESTHER BARTSCH

GOETHE UNIVERSITY FRANKFURT

WORKSHOP ON THE QCD EQUATION OF STATE IN DENSE
MATTER HIC AND ASTROPHYSICS – MAGIC23, KOVALAM

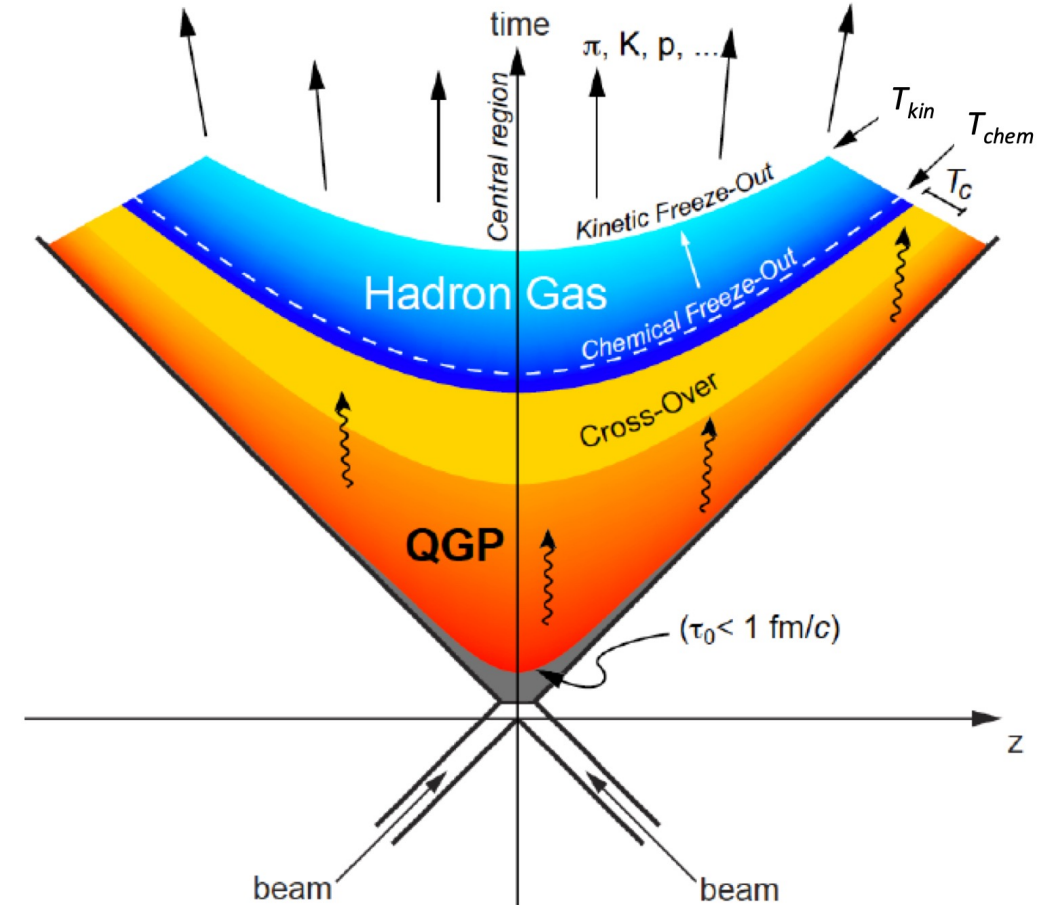
Nuclear matter production

- In high-energy hadronic collisions a deconfined phase of strongly interacting matter in equilibrium is created: quark-gluon plasma (QGP)
- The system expands and cools down
 - When $T < T_c$: Transition to a gas of interacting hadrons and resonances
 - Chemical freeze-out temperature T_{ch} (~ 155 MeV): Inelastic interactions stop and hadron yields are fixed
 - Kinetic freeze-out temperature T_{kin} (~ 110 MeV): Elastic interactions stop and particle momentum distributions are fixed



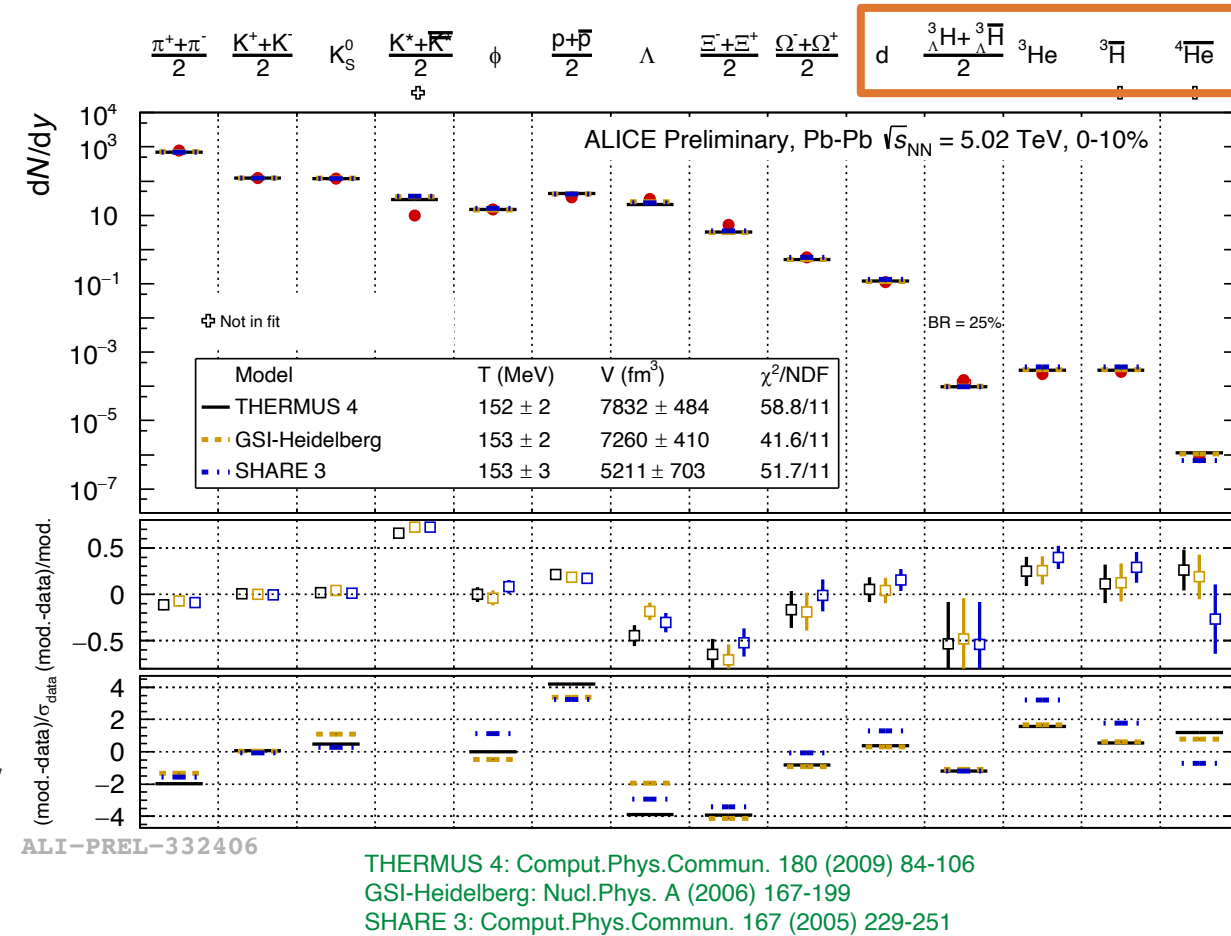
Nuclear matter production

- Light (anti)(hyper)nuclei are abundantly produced at the LHC in pp, p—Pb and Pb—Pb collisions
- The production mechanism in high-energy physics is still not completely understood
- Two classes of models on the market to describe nuclei production:
 - Statistical hadronization models (SHM)
 T_{ch} relevant
production scales with particle mass
 - Coalescence models (CM)
 T_{kin} relevant
production rates driven by the ratio between the particle radius and the system size

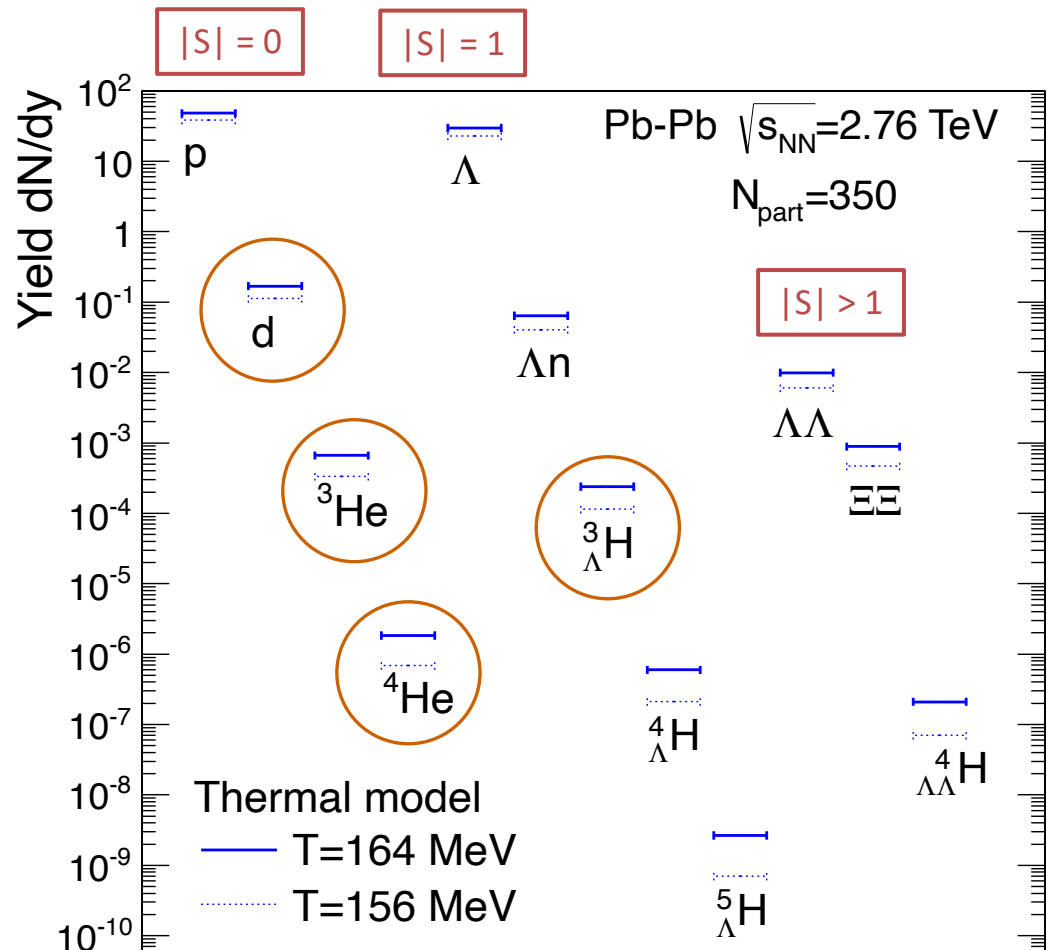


Statistical hadronization

- In Pb–Pb collisions the system can be described by a **grand canonical ensemble** with three free parameters (μ_B , V and T_{ch})
→ Quantum numbers are conserved on average
- ALICE Pb–Pb data compared to Statistical Hadronization Model fit
→ Very good agreement
- In small systems a **canonical ensemble** (CSM) has to be applied (free parameters N , V , T_{ch})
→ Quantum numbers are conserved exactly
V. Vovchenko, B. Dönigus, and H. Stoecker, Phys. Rev. C 100 (2019) 054906
- Particles and antiparticles are produced equally at the LHC ($\mu_B \approx 0$)



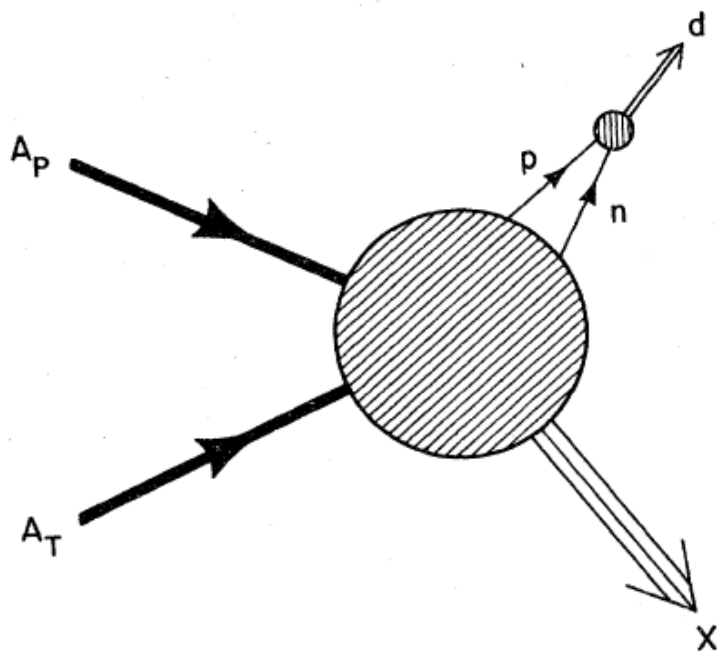
Production of light (hyper)nuclei



A. Andronic, private communication, model based on:
Phys. Lett. B 697 (2011) 203

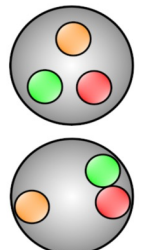
- Abundance of nuclei strongly sensitive to chemical freeze-out temperature T_{ch} , due to
 - Large mass
 - Exponential dependence of the yield $\sim e^{(-m/T_{\text{ch}})}$
- Note: Binding energy of nuclei (few MeV) small compared to T_{ch}

Coalescence model

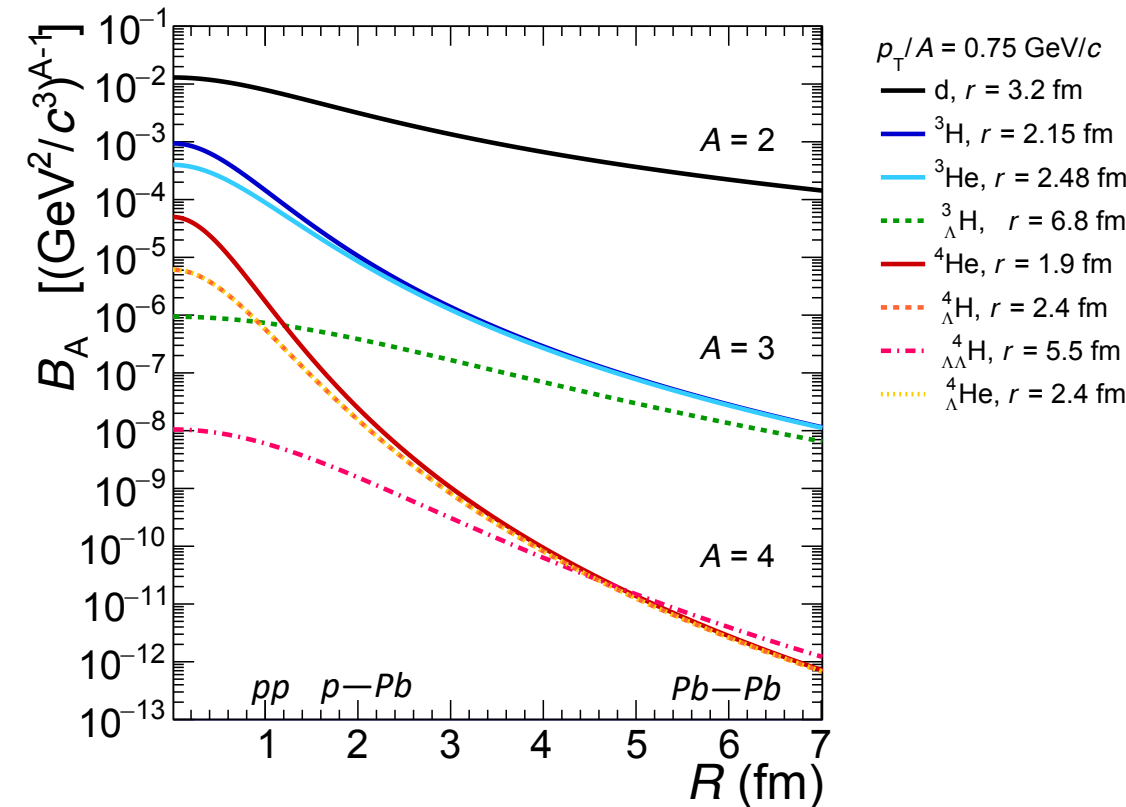


J. I. Kapusta, Phys. Rev. C 21 (1980) 1301

- Nuclei are formed after kinetic freeze-out by protons and neutrons which are nearby in space and have similar velocities
 - Production rate is connected to the size of the bound state relative to the system size
- Advanced models use quantum mechanical approximation
 - Wigner formalism is used
 - Wave functions of the constituents are multiplied with a probability distribution that a nucleus is formed
- Differentiation for $A \geq 3$
 - Three-body coalescence: All nucleons in the nucleus have the same distance
 - Two-body coalescence: Inner structure of the nucleus is taken into account



Coalescence parameter



F. Bellini, and A. Kalweit, Acta Phys. Pol. B 50 (2019) 991

- Main parameter of the coalescence model B_A :

$$B_A = \frac{E_A \frac{d^3N_A}{d^3p_A}}{\left(E_p \frac{d^3N_p}{d^3p_p} \right)^A}$$

A : mass number of nucleus
 $p_p = p_A/A$

- B_A is related to the probability to form a nucleus via coalescence

ALICE detector setup

Inner Tracking System (ITS)

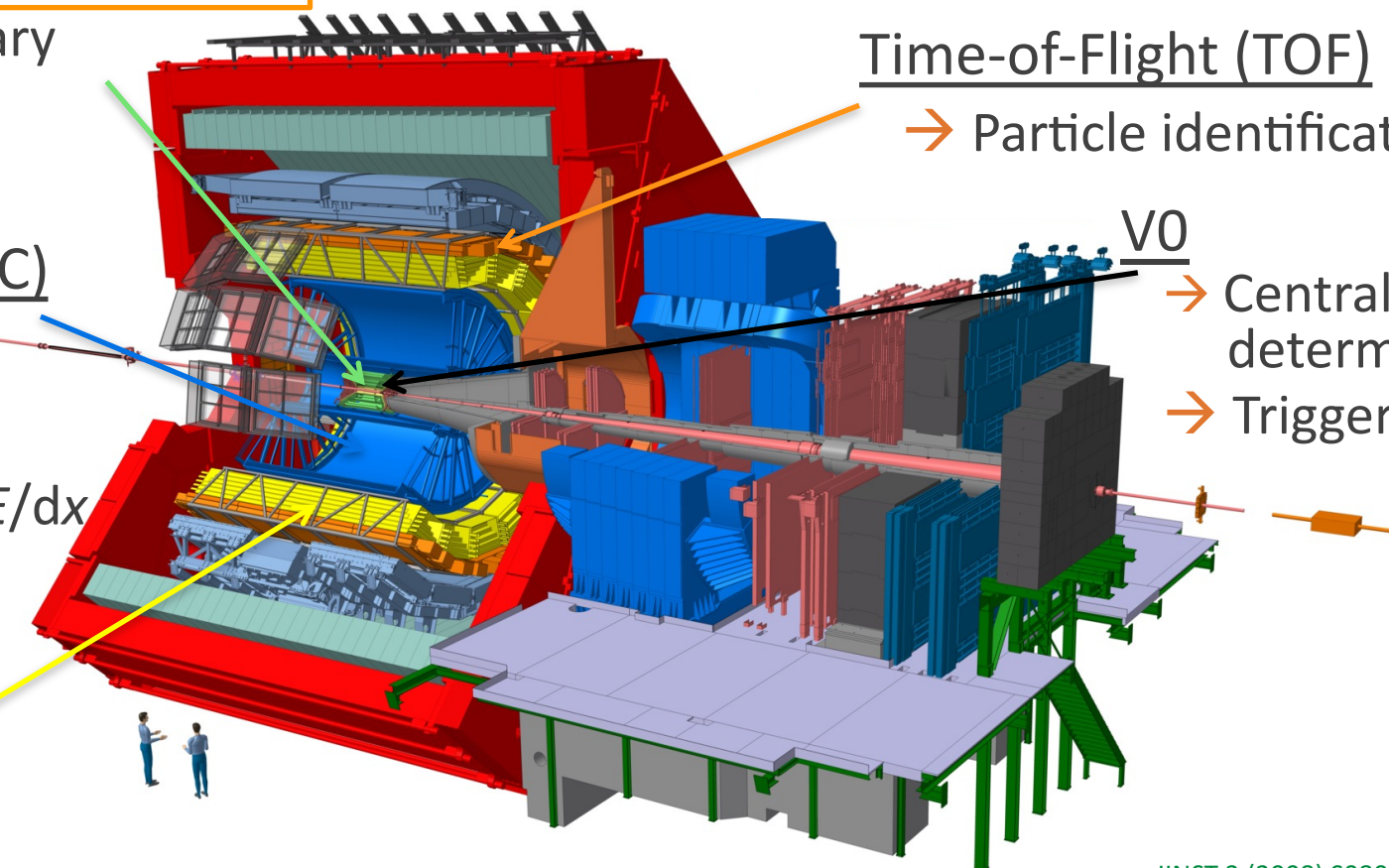
- Vertexing
- Separation between primary and secondary vertices
- Tracking

$$\sigma_{\text{DCA}_{xy}} < 100 \mu\text{m} \text{ in Pb—Pb}$$

Time Projection Chamber (TPC)

- Tracking
- Vertexing
- Particle identification via dE/dx

$$\frac{\sigma(dE/dx)}{dE/dx} \approx 6 \%$$



Time-of-Flight (TOF)

- Particle identification

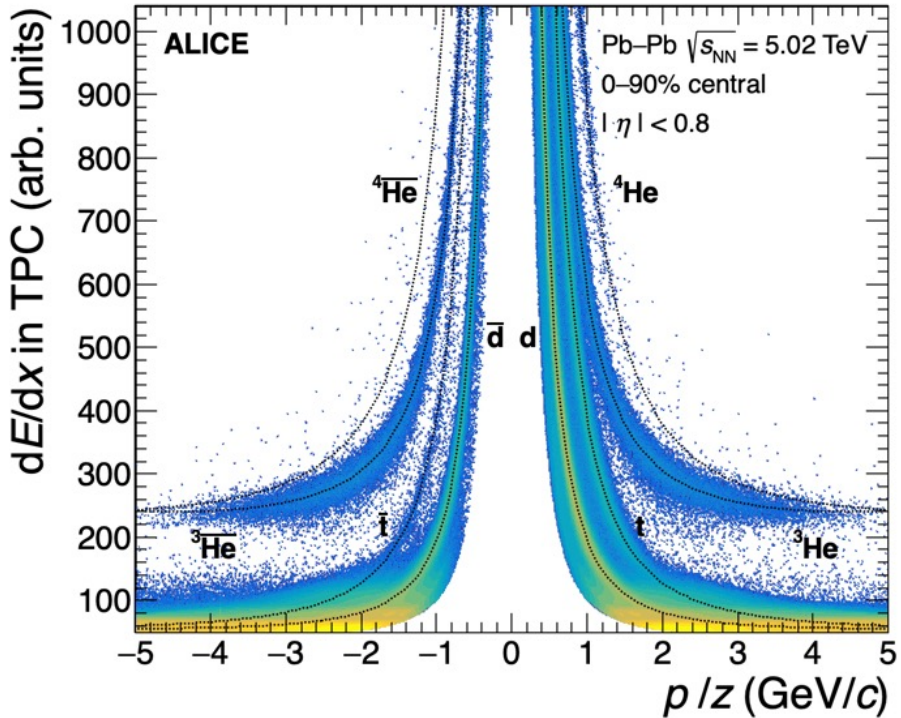
$$\sigma_{\text{TOF}} \approx 60 \text{ ps} \text{ in Pb—Pb}$$

Transition Radiation Detector (TRD)

- Tracking

JINST 3 (2008) S08002

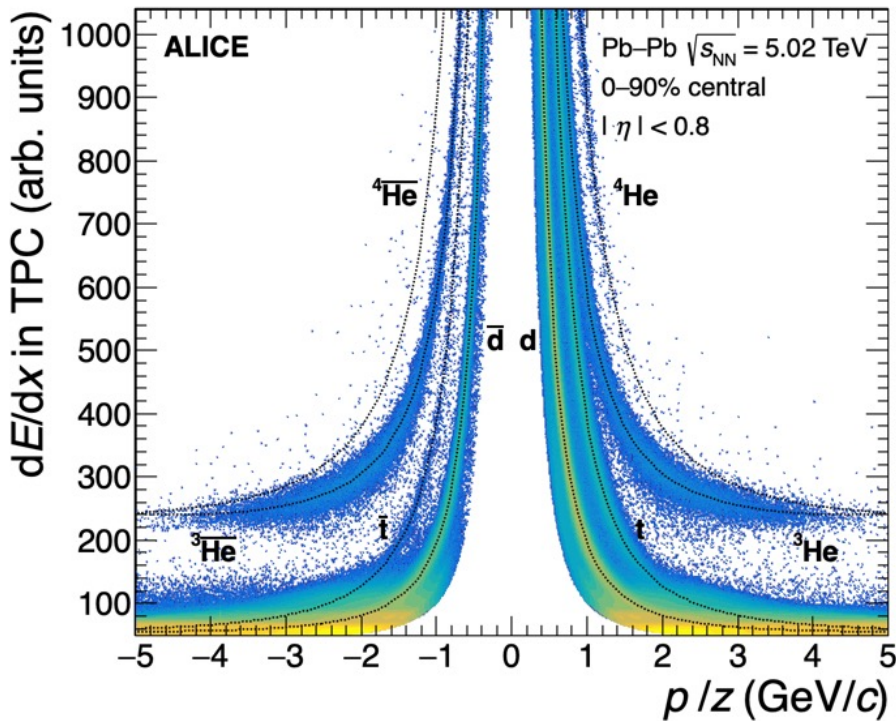
Nuclei identification



- Low momenta: TPC
→ Nuclei identified using the **energy loss** measurement

ALICE Collaboration, arXiv:2211.14015 [nucl-ex]

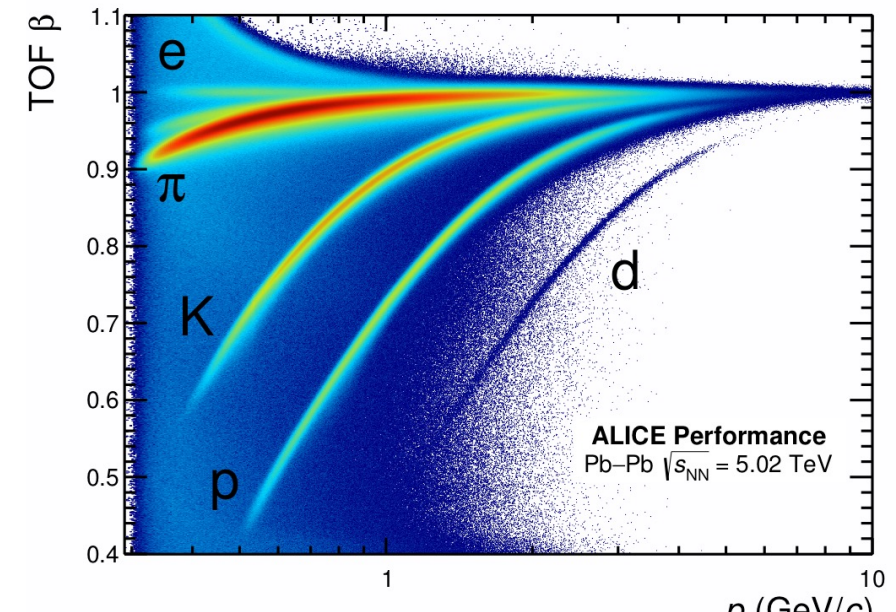
Nuclei identification



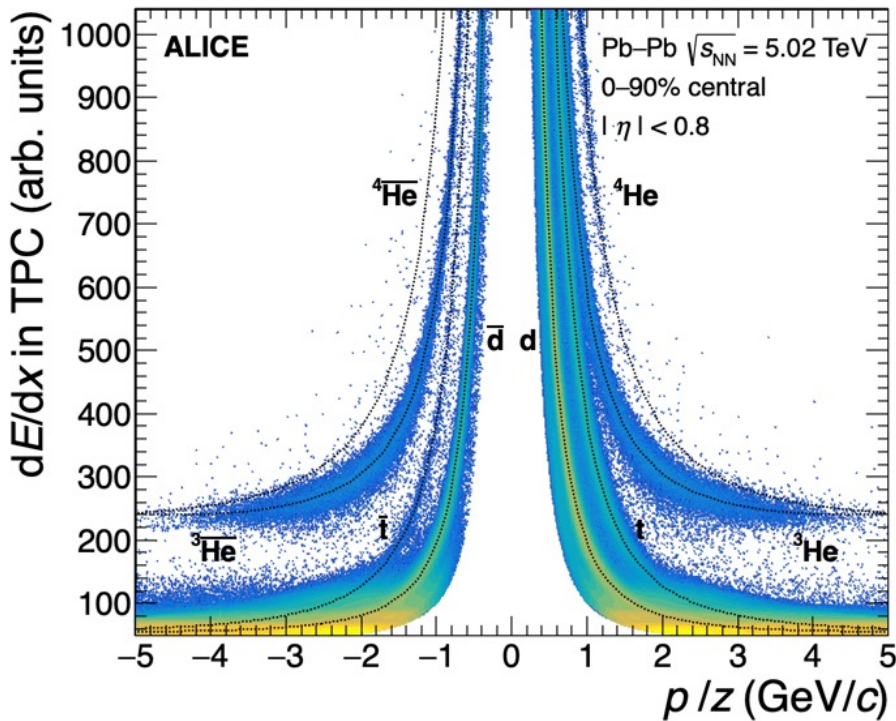
- Low momenta: TPC
→ Nuclei identified using the **energy loss** measurement
- Momentum determined from track curvature
- High momenta: TOF

$$\frac{p}{z} = r B$$

$$\beta = \frac{L}{t_{TOF}c}$$



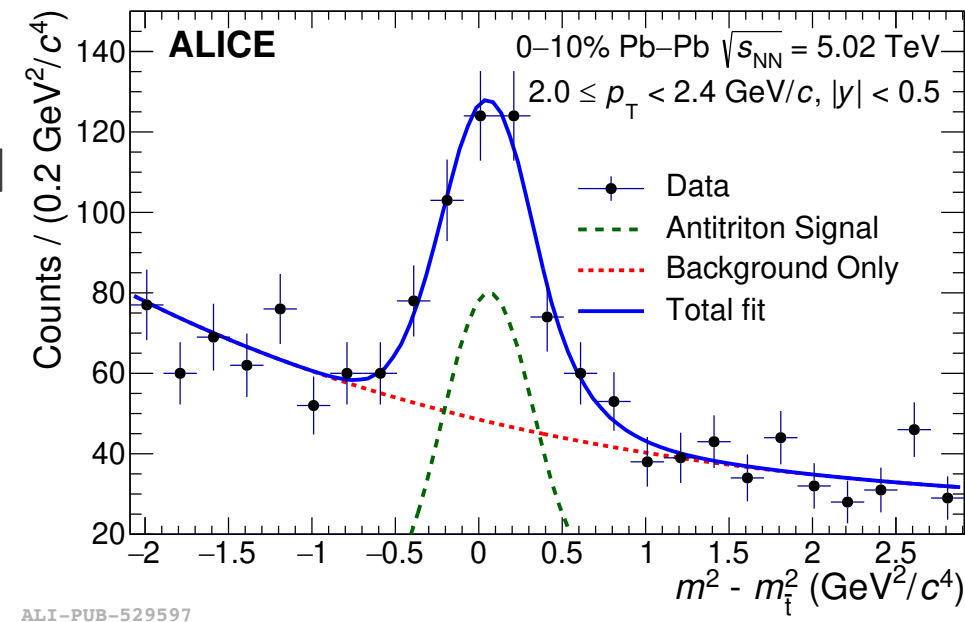
Nuclei identification



ALICE Collaboration, arXiv:2211.14015 [nucl-ex]

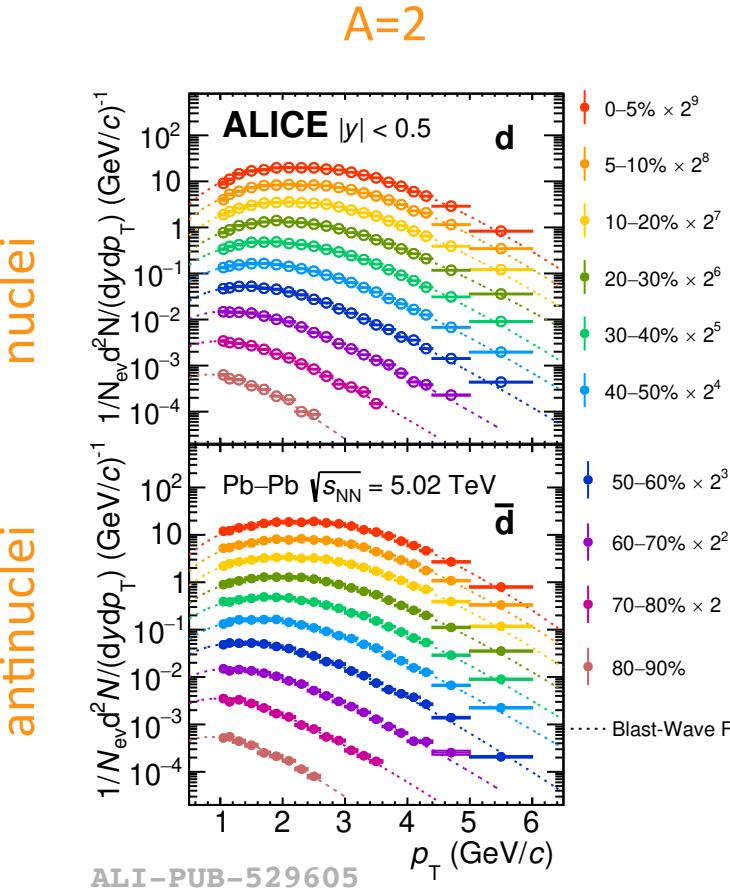
- Low momenta: TPC
→ Nuclei identified using the **energy loss** measurement
- Momentum determined from track curvature
$$\frac{p}{z} = r B$$
- High momenta: TOF
→ m^2 distribution is calculated from the **time-of-flight** measurement

$$m^2 = \frac{(1-\beta^2)}{\beta^2} p^2$$

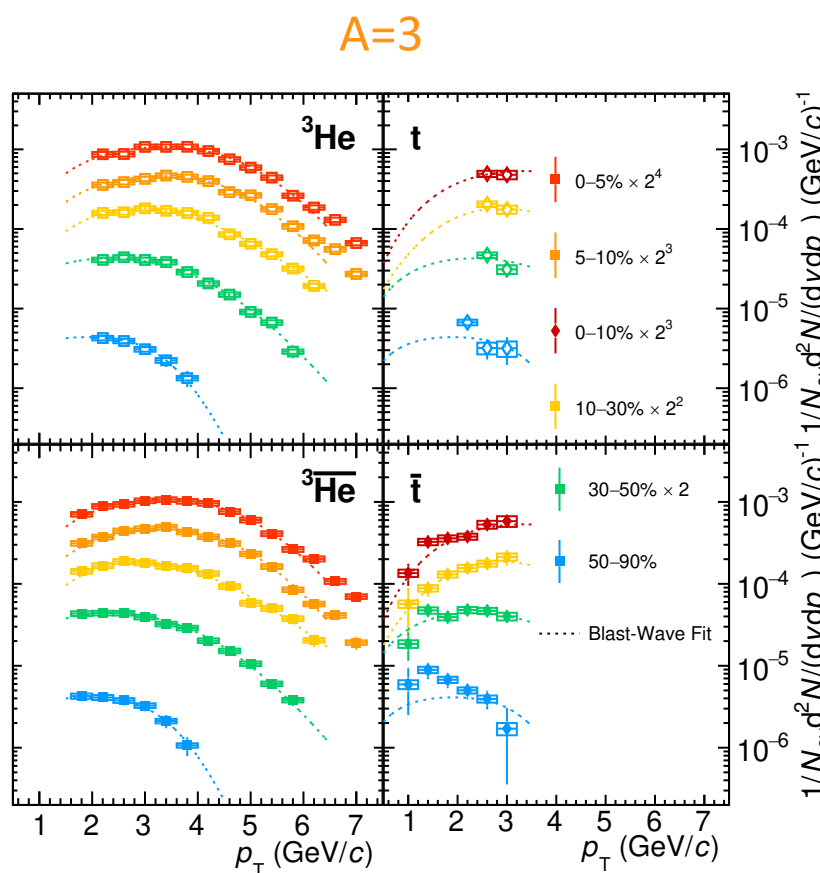


ALICE Collaboration, arXiv:2211.14015 [nucl-ex]

Nuclei p_T spectra in Pb—Pb at $\sqrt{s_{NN}}=5$ TeV



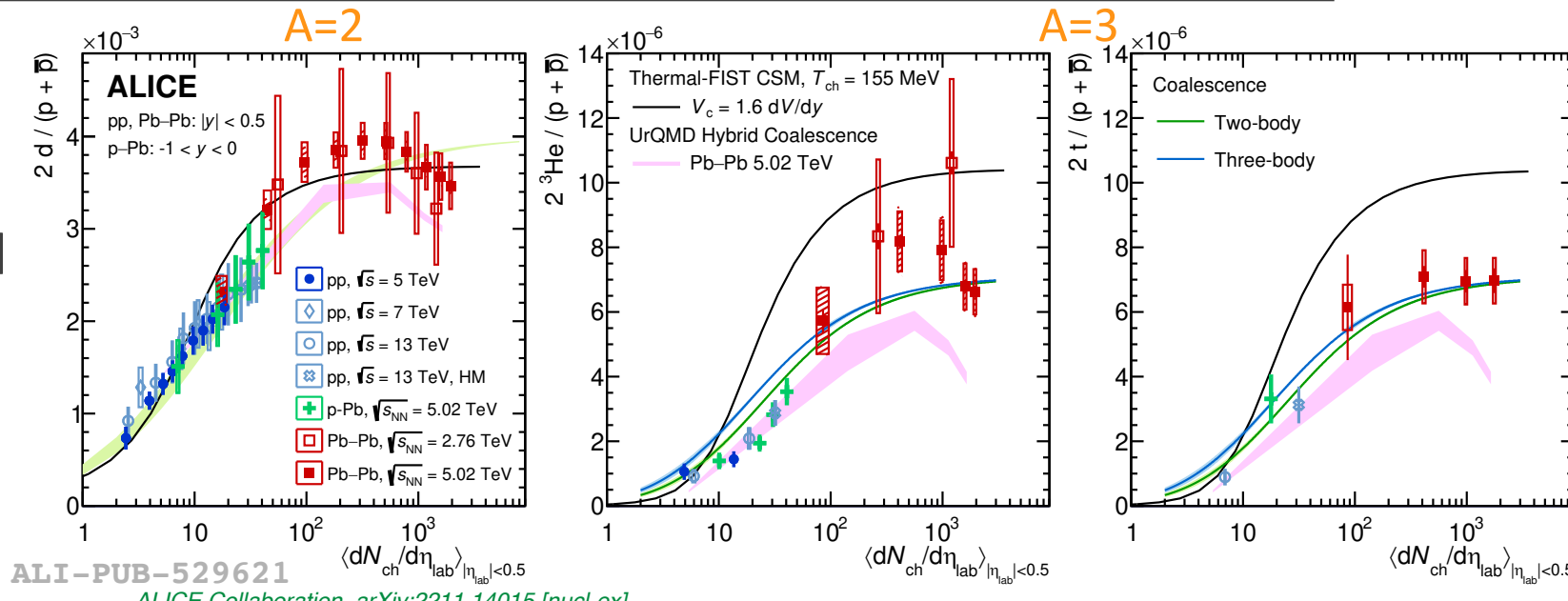
ALICE Collaboration, arXiv:2211.14015 [nucl-ex]



- $A=2$ and $A=3$ (anti)nuclei measured in Pb—Pb collisions at $\sqrt{s_{NN}} = 5$ TeV in different centrality intervals.
- Nuclei and antinuclei compatible
- Hardening of the spectra
→ Average p_T nearly doubling going from peripheral to central collisions
- Production yields (dN/dy) extracted by integrating the spectra and extrapolating to zero and high p_T through a fit with a Blast-Wave function

Nuclei-over-proton ratio

- Clear increasing trend from pp to p–Pb and saturation in Pb–Pb collisions can be observed
- Data compared to CSM, Analytical Coalescence and UrQMD Hybrid Coalescence models
- All three models describe the data qualitatively but have problems describing it quantitatively
- For deuterons all models do rather good, for A=3 (in particular for tritons) coalescence is closer to the data with respect to the CSM



ALICE Collaboration, arXiv:2211.14015 [nucl-ex]

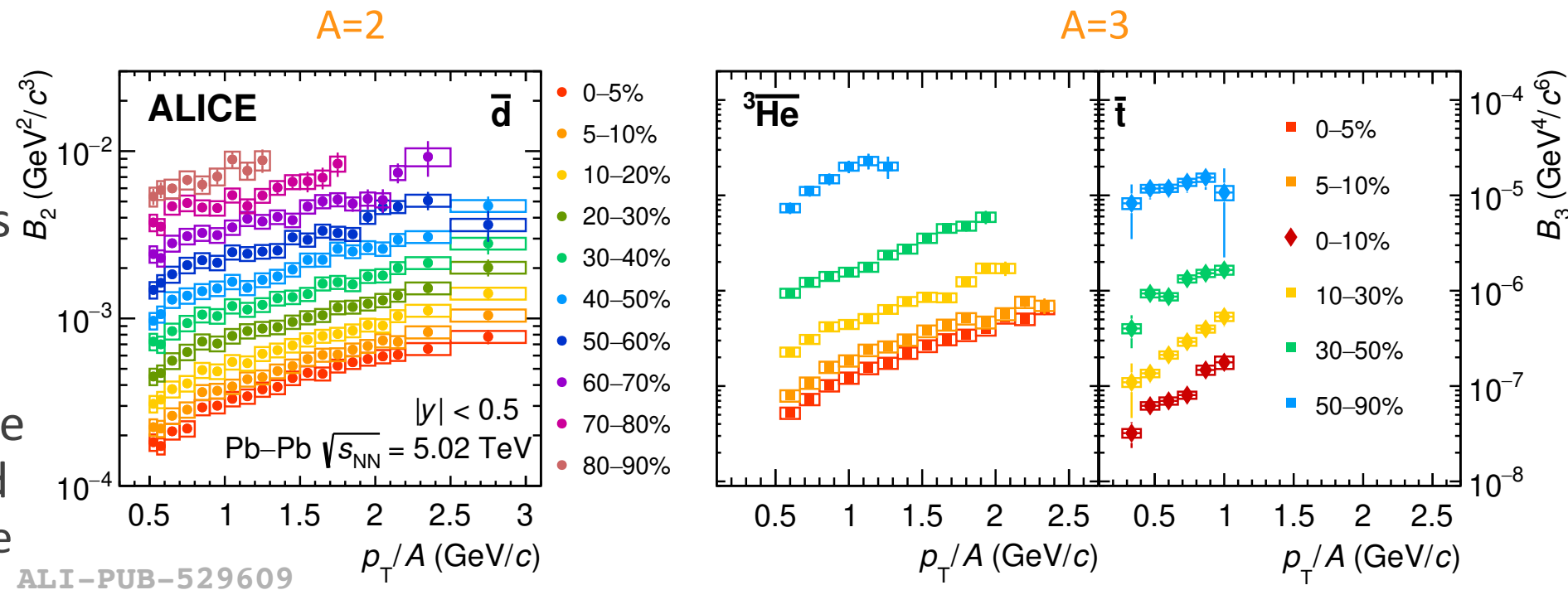
CSM: V. Vovchenko, B. Döningus, and H. Stoecker, Phys. Lett. B 785 (2018) 171–174, arXiv:1808.05245 [hep-ph]

Coalescence: K.-J. Sun, C. M. Ko, and B. Döningus, , Phys. Lett. B 792 (2019) 132–137, arXiv:1812.05175 [nucl-th]

UrQMD: T. Reichert, J. Steinheimer, V. Vovchenko, B. Döningus, and M. Bleicher, Phys. Rev. C 107 (2023) 014912, arXiv:2210.11876 [nucl-th]

Coalescence parameters B_2 and B_3

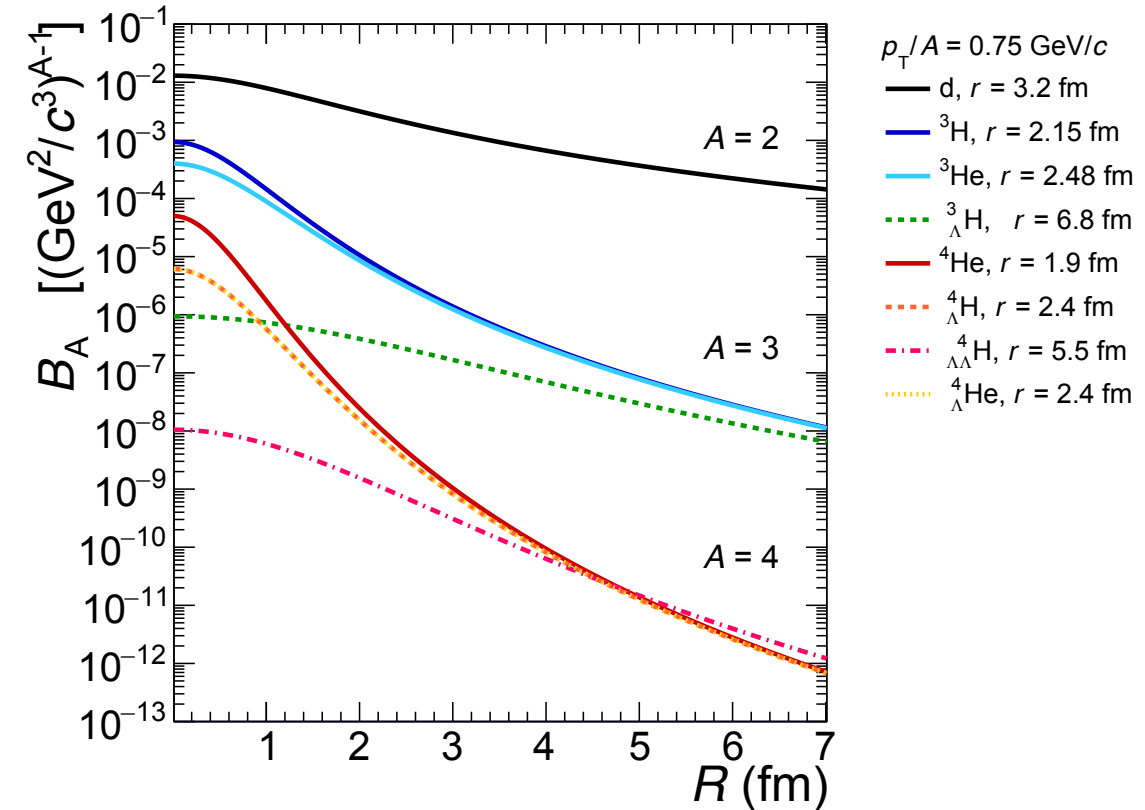
- B_A is larger for peripheral collisions where the system size and thus the configuration space is smaller
- In Pb–Pb collisions a rise of B_A with p_T is observed
→ For high p_T particles the configuration space becomes smaller due to a smaller region of source homogeneity
- Moving from central to more peripheral collisions (i.e. towards lower multiplicities) the rise in p_T becomes milder



ALICE Collaboration, arXiv:2211.14015 [nucl-ex]

t-over- ${}^3\text{He}$ ratio in small systems

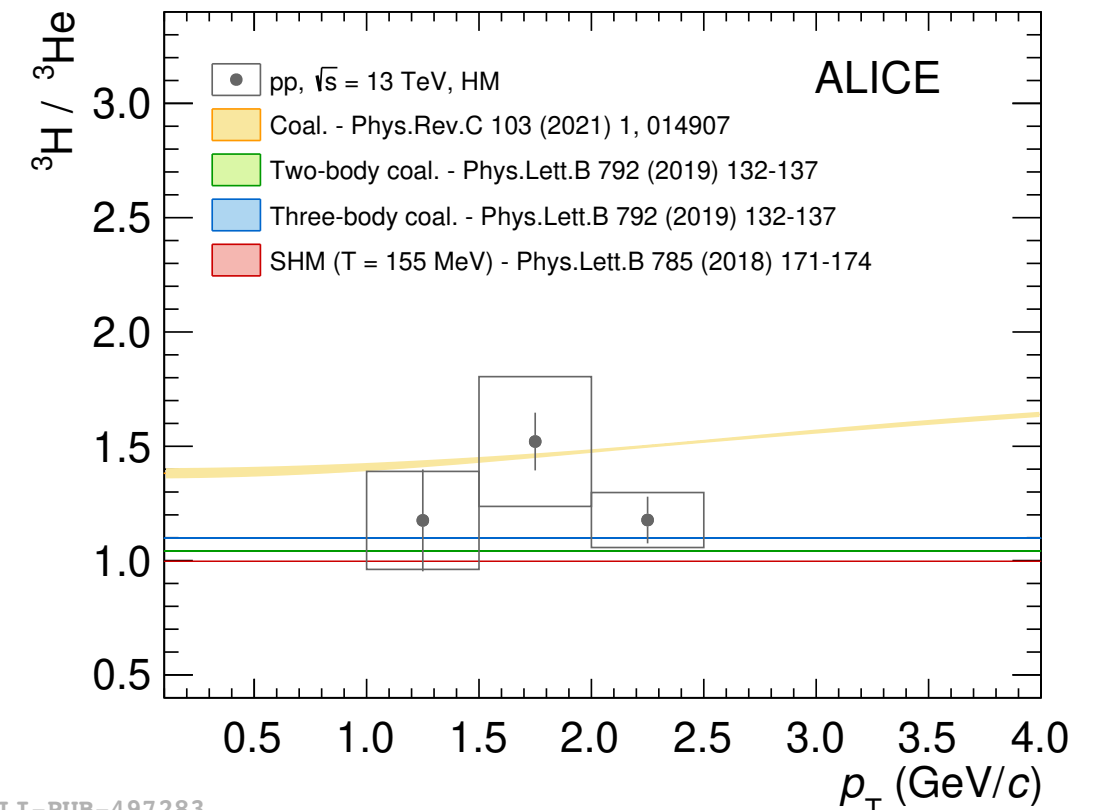
- Coalescence predicts ${}^3\text{H}/{}^3\text{He} > 1$ in small systems due to different nuclei radii
→ $r {}^3\text{H}/r {}^3\text{He} \approx 0.9$
- SHM expectation of this ratio is close to unity due to a similar mass of both nuclei



F. Bellini, and A. Kalweit, Acta Phys. Pol. B 50 (2019) 991

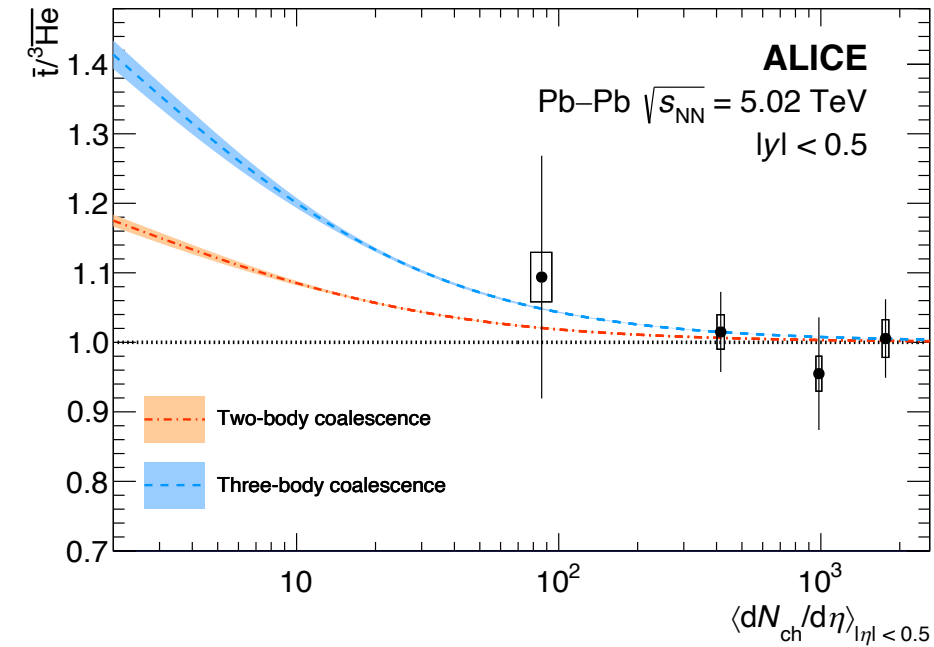
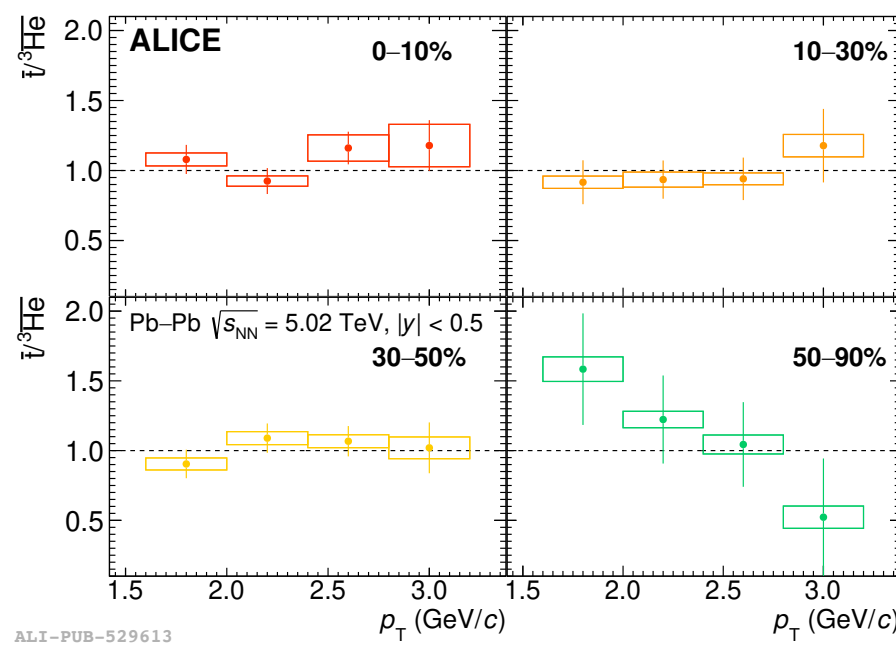
t-over- ${}^3\text{He}$ ratio in small systems

- Coalescence predicts ${}^3\text{H}/{}^3\text{He} > 1$ in small systems due to different nuclei radii
 $\rightarrow r_{{}^3\text{H}}/r_{{}^3\text{He}} \approx 0.9$
- SHM expectation of this ratio is close to unity due to a similar mass of both nuclei
- Ratio of transverse momentum spectra of t and ${}^3\text{He}$ in high-multiplicity pp collisions at $\sqrt{s} = 13 \text{ TeV}$
- Flat in p_T and within uncertainties compatible with unity



ALICE Collaboration, JHEP 01 (2022) 106

\bar{t} -over- ${}^3\text{He}$ ratio in Pb—Pb collisions



ALICE Collaboration, arXiv:2211.14015 [nucl-ex]

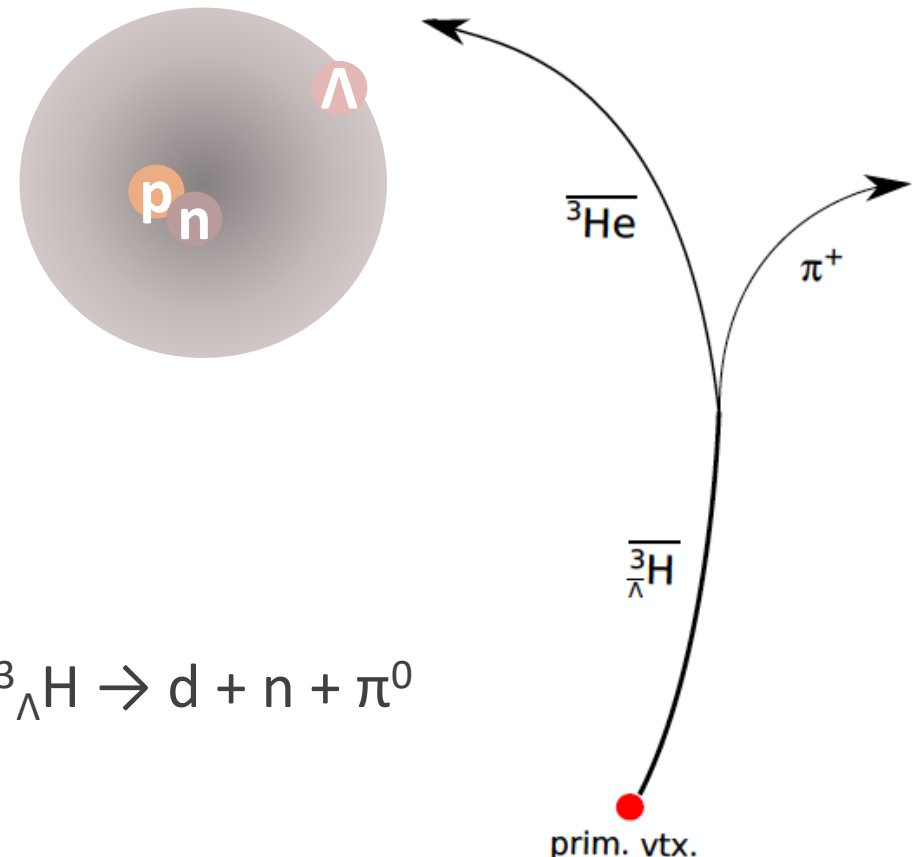
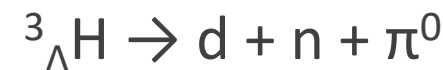
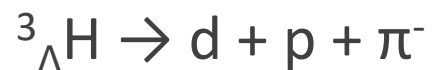
Coalescence: K.-J. Sun, C. M. Ko, and B. Dönigus, Phys. Lett. B 792 (2019) 132–137, arXiv:1812.05175 [nucl-th]

- Ratio of transverse momentum spectra of \bar{t} and ${}^3\text{He}$ in different centrality intervals in Pb—Pb collisions at $\sqrt{s_{\text{NN}}} = 5 \text{ TeV}$
- Flat in p_{T} and within uncertainties compatible with unity

- Average \bar{t} over ${}^3\text{He}$ ratio versus multiplicity compared to two-body and three-body coal.
- Present data not yet conclusive
→ will be addressed with high precision in LHC Run 3

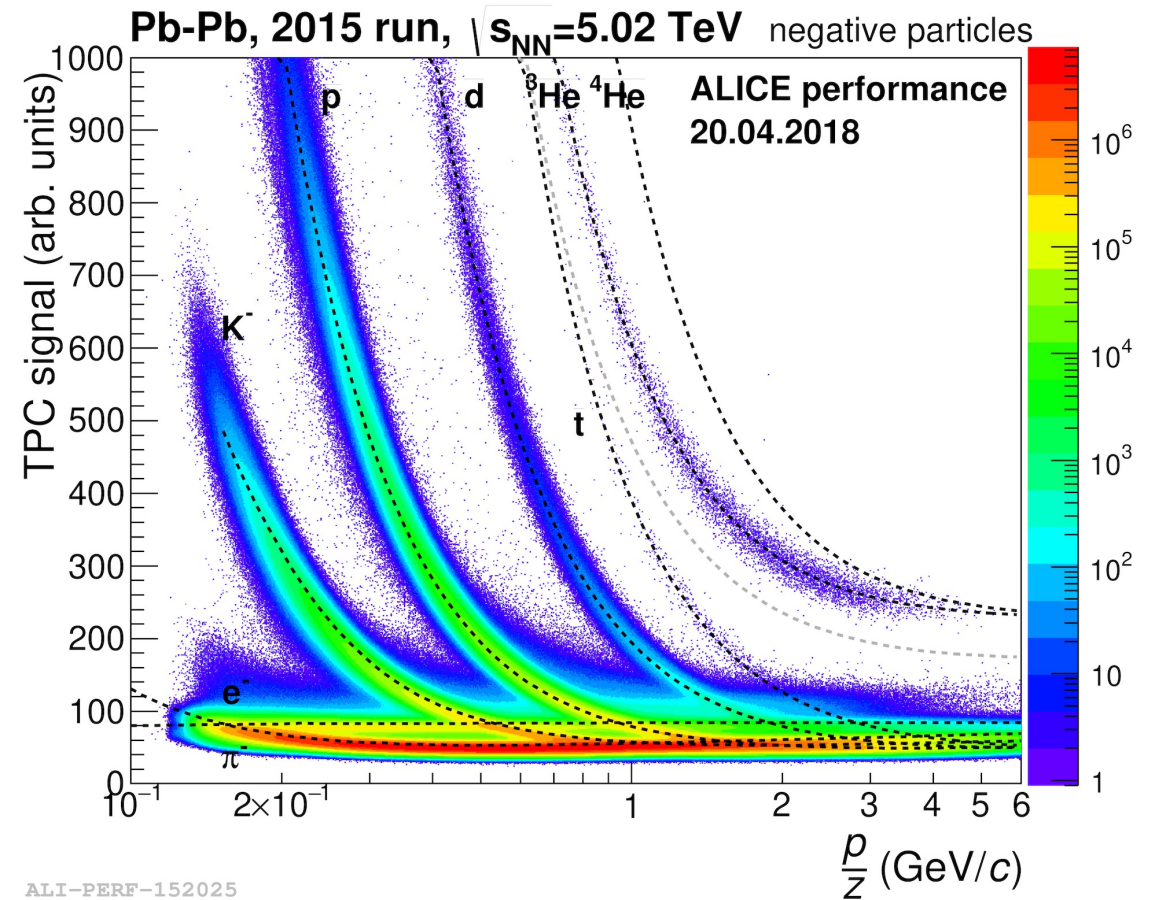
Hypertriton

- Bound state of Λ , p and n
- Lightest bound hypernucleus ($m \approx 2.991 \text{ GeV}/c^2$) and very low Λ separation energy ($\approx 130 \text{ keV}$)
- Recent calculations predict a large radius for the hypertriton wave function $r_{\Lambda-d} = 10.79^{+3.04}_{-1.53} \text{ fm}$
F. Hildebrand, H.-W. Hammer, Phys. Rev. C 100 (2019) 034002, arXiv:1904.05818[nucl-th]
- Hypertriton decays weakly after a few cm
- Decay modes:



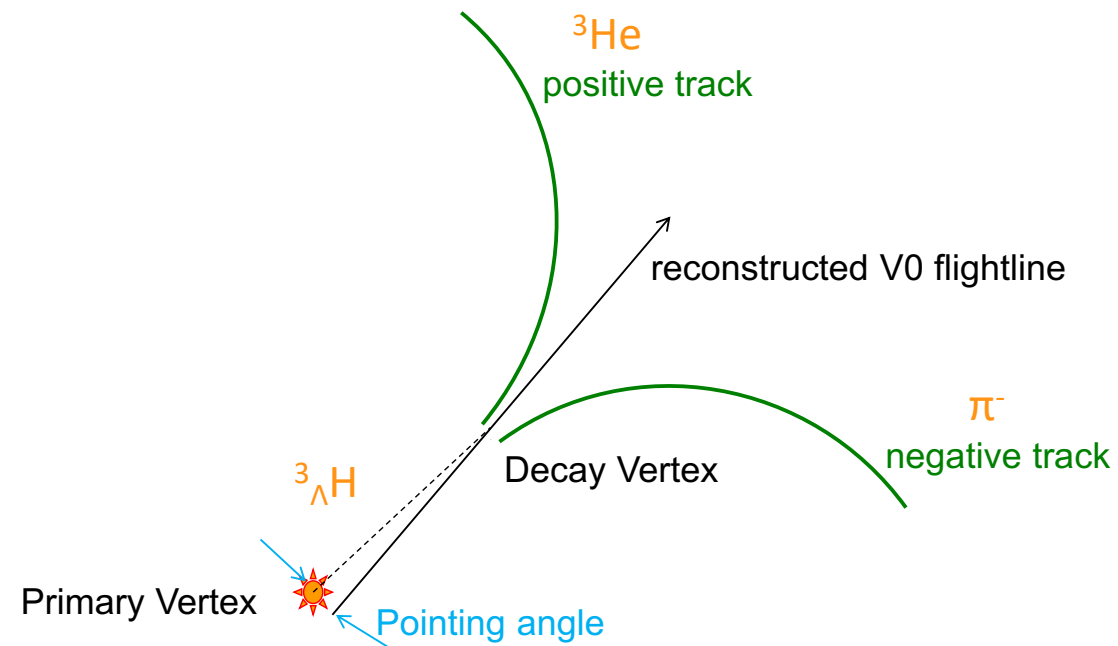
Hypertriton reconstruction

- **Step 1:** find and identify the daughter particle tracks
 - Using TPC PID via the specific energy loss
 - Excellent separation of different particle species



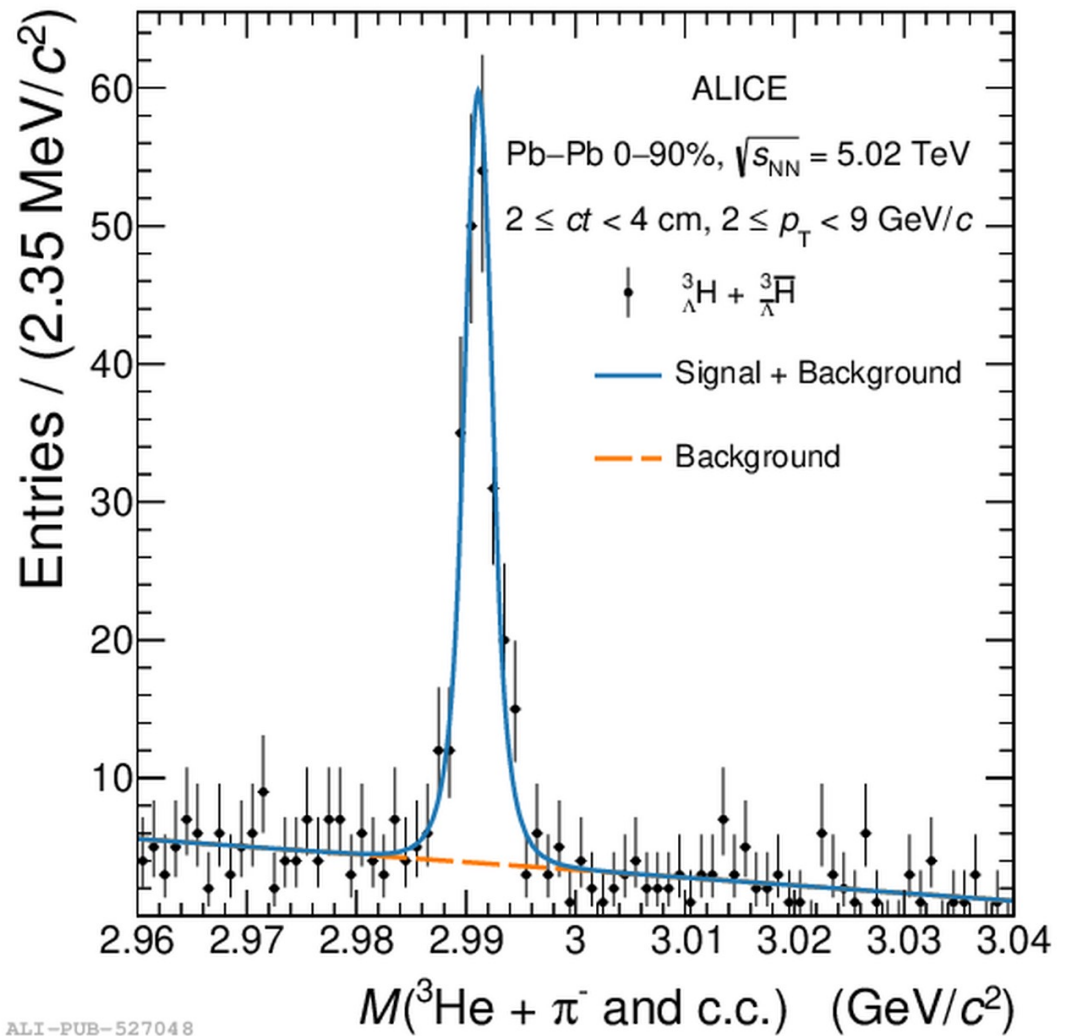
Hypertriton reconstruction

- Step 1: find and identify the daughter particle tracks
- Step 2: reconstruct the decay vertex of the hypertriton
 - The identified daughters are assumed to come from a **common vertex**
 - Their tracks are matched by algorithms to find the **best possible decay vertex**
 - **Problem:** huge combinatorial background
 - **Solution:** topological and kinematical cuts or machine learning approach



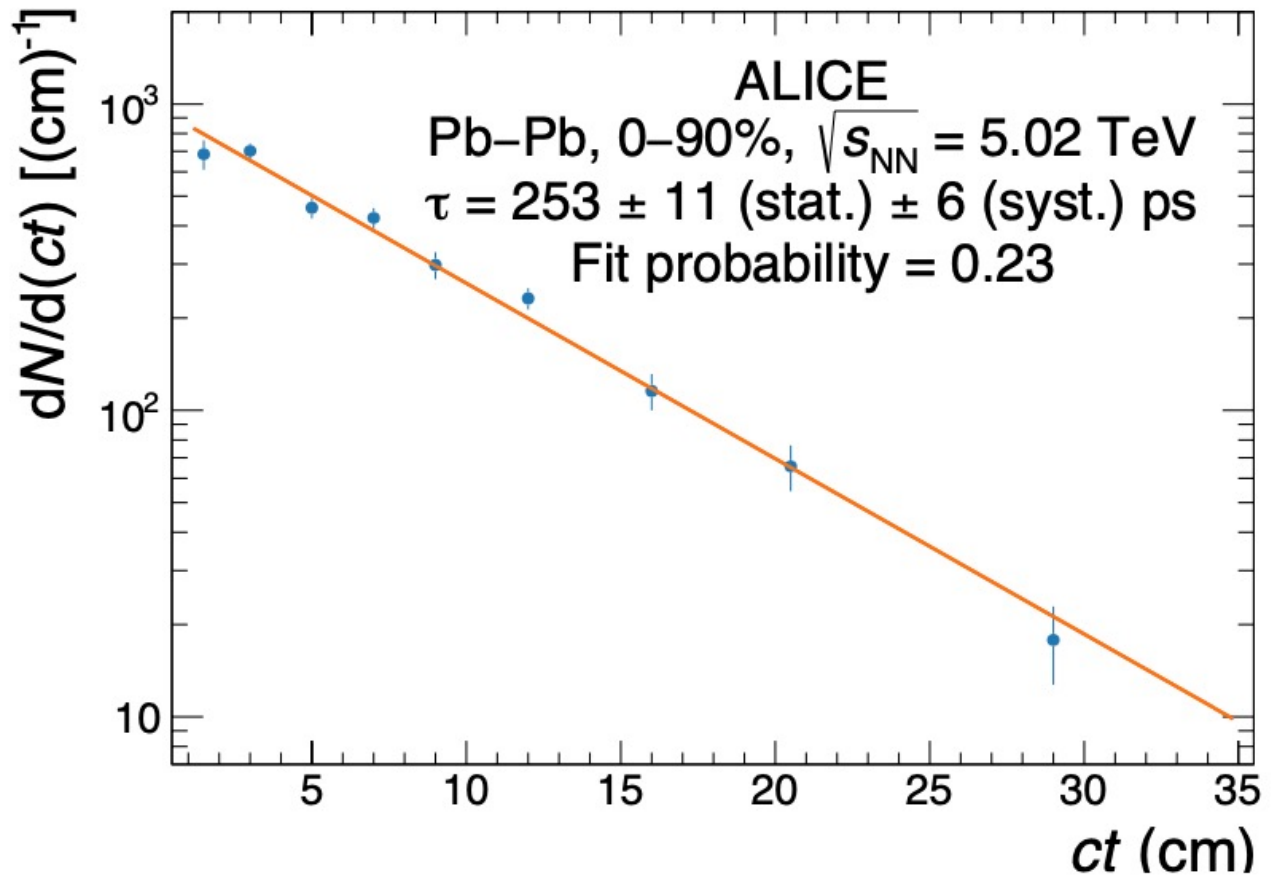
Hypertriton in Pb—Pb collisions

- Recent measurement in Run 2 Pb—Pb collisions at 5.02 TeV
- Signal extraction by using a machine learning approach
- Using a boosted decision tree (BDT) and hyper parameter optimisation



Hypertriton lifetime

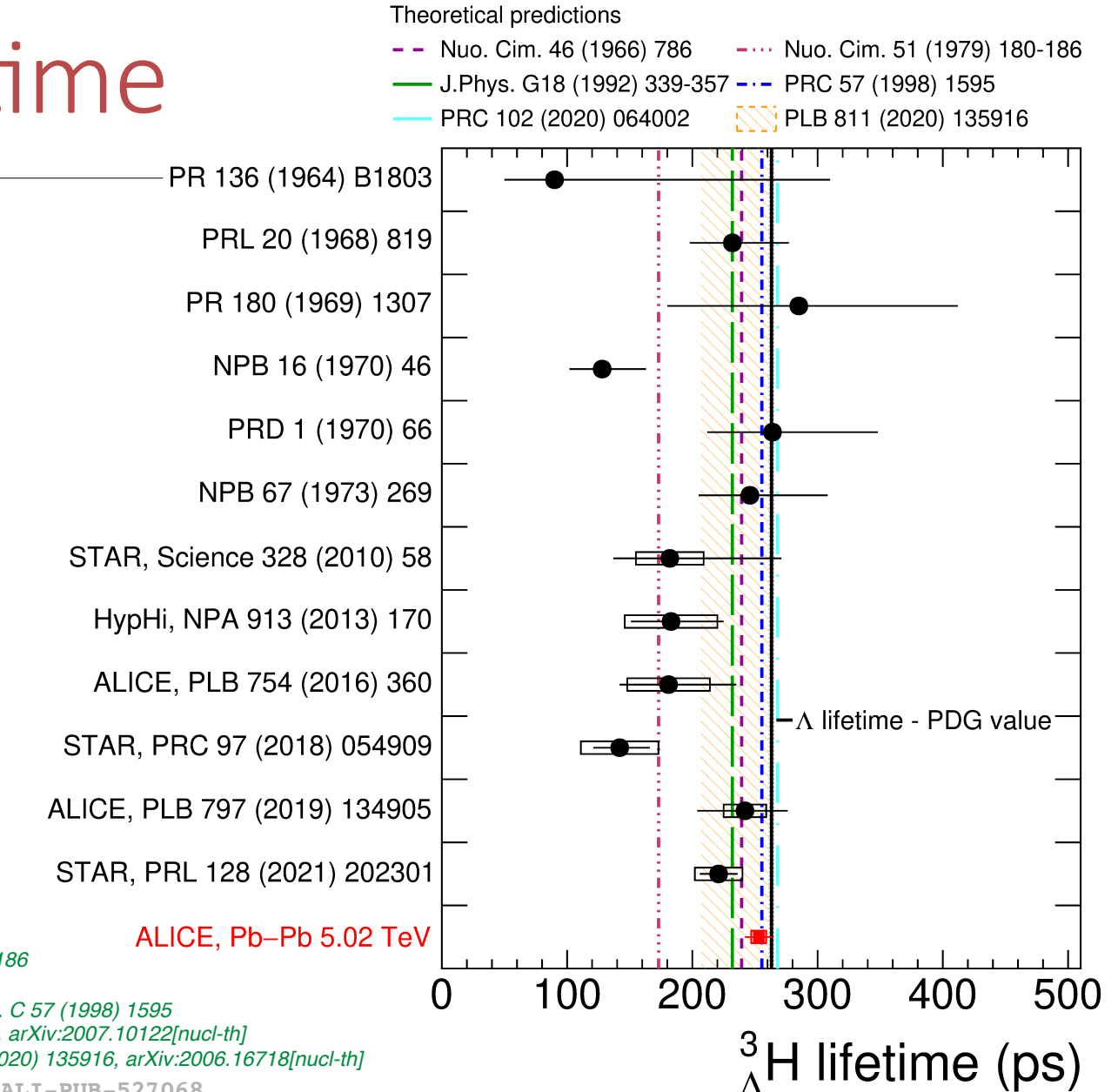
- (Anti)hypertriton signal split in 9 ct bins
- Exponential decay spectrum shown with statistical uncertainties and best fit to the measurement
- Most precise measurement of the hypertriton lifetime to date



ALICE Collaboration, arXiv:2209.07360 [nucl-ex]

Hypertriton lifetime

- Hypertriton lifetime is compatible with the free Λ lifetime within its uncertainties
→ Supports a very loosely-bound state
- New result increased the world average lifetime value



ALICE Collaboration, arXiv:2209.07360 [nucl-ex]

[Nuo. Cim. 46 (1966) 786] M. Rayet, and R. H. Dalitz, Nuovo Cim. A46 (1966) 786-794

[Nuo. Cim. 51 (1979) 180-186] H. M. M. Mansour, and K. Higgins, Nuovo Cim. A51 (1979) 180-186

[J.Phys G18 (1992) 339-357] J. G. Congleton, J. Phys. G 18 (1992) 339-357

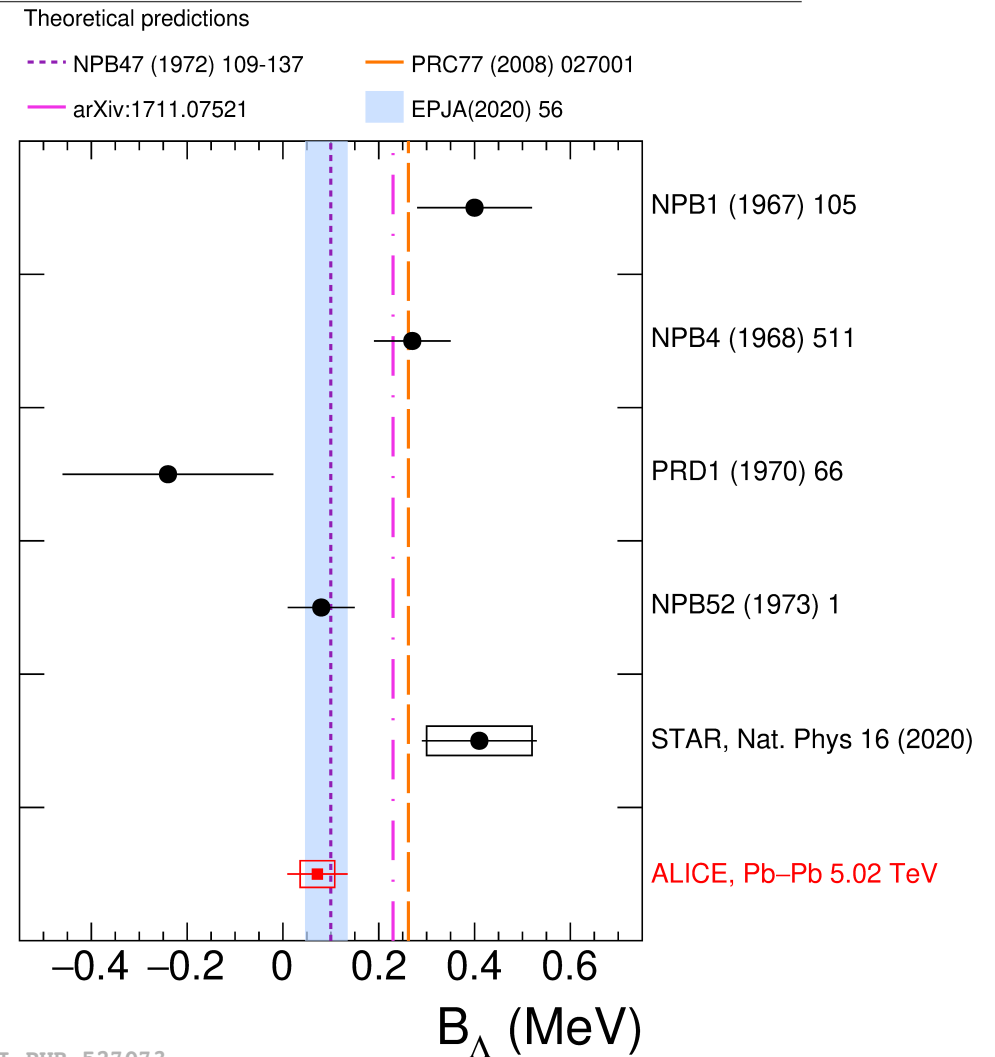
[PRC 57(1998) 1595] H. Kamada, J. Golak, K. Miyagawa, H. Witała, and W. Glöckle, Phys. Rev. C 57 (1998) 1595

[PRC 102 (2020) 064002] F. Hildenbrand and H.-W. Hammer, Phys. Rev. C 102 (2020) 064002, arXiv:2007.10122[nucl-th]

[PLB 811 (2020) 135916] A.Pérez-Obiol, D.Gazda, E.Friedman, and A Gal, Phys. Lett. B 811 (2020) 135916, arXiv:2006.16718[nucl-th]

Hypertriton: Λ separation energy

- ALICE measurement of the hypertriton binding energy is compatible with the latest theoretical predictions.



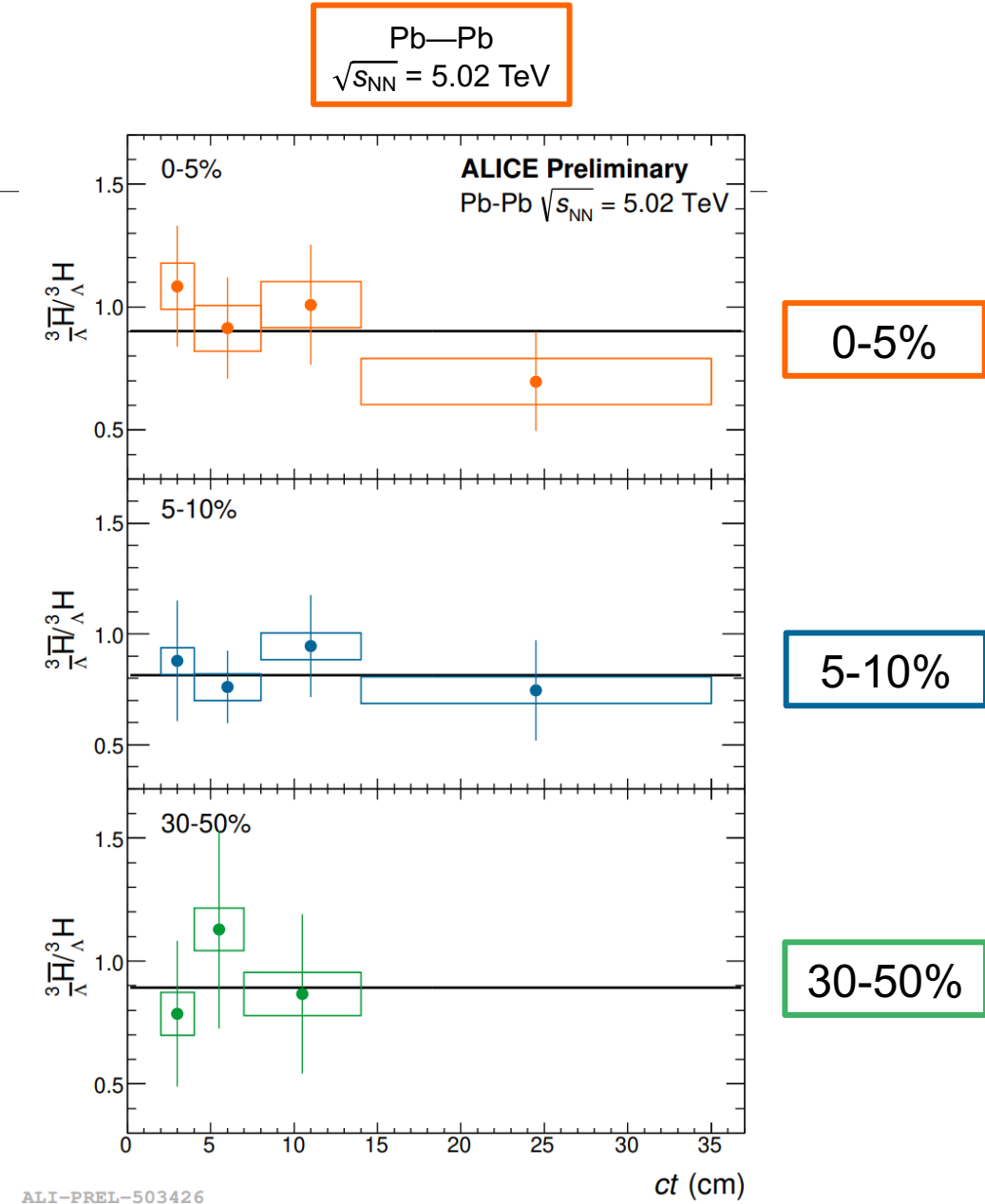
ALICE Collaboration, arXiv:2209.07360 [nucl-ex]
[NPB47(1972)] R.H. Dalitz, R.C. Herndon, Y.C. Tang, Nuclear Physics B 47 (1972) 109-137
[arXiv:1711.07521] D. Lonardoni, and F. Pederiva, arXiv:1711.07521 [nucl-th]
[PRC77(2008)] Y. Fujiwara, Y. Suzuki, M. Kohno, and K. Miyagawa., Phys. Rev. C 77 (2008) 027001
[EPJA(2020) 56] F. Hildenbrand and H.-W. Hammer, Phys. Rev. C 100 (2019) 034002, arXiv:1904.05818[nucl-th]

ALI-PUB-527073

Hypertriton production

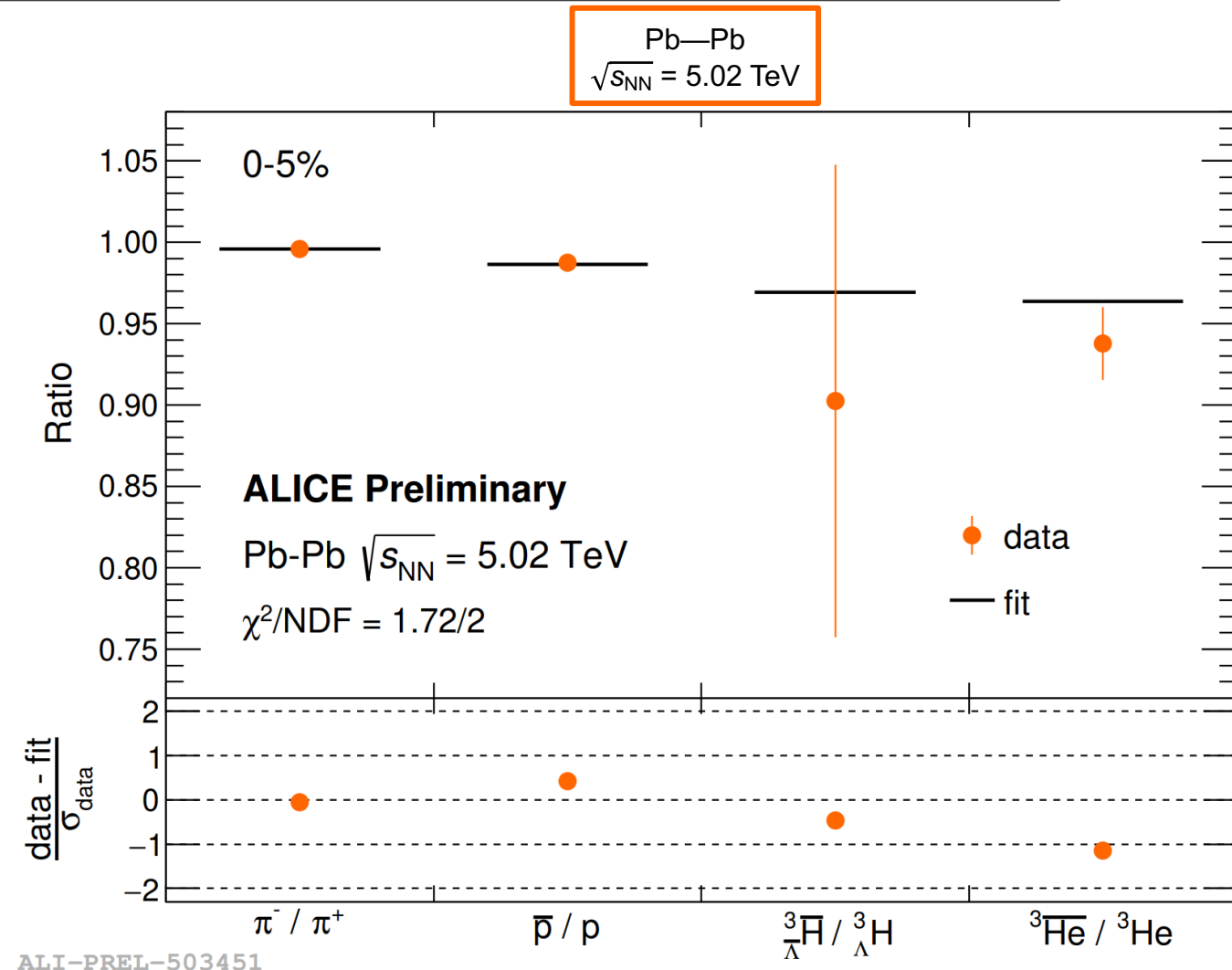
- Determination of the baryochemical potential including the hypertriton in different centrality intervals
- Using antiparticle to particle ratios as input
- Nuclei lead to higher sensitivity due to larger amount of baryons

$$\bar{h}/h \propto \exp \left[-2 \left(B + \frac{S}{3} \right) \frac{\mu_B}{T} - 2I_3 \frac{\mu_{I_3}}{T} \right]$$



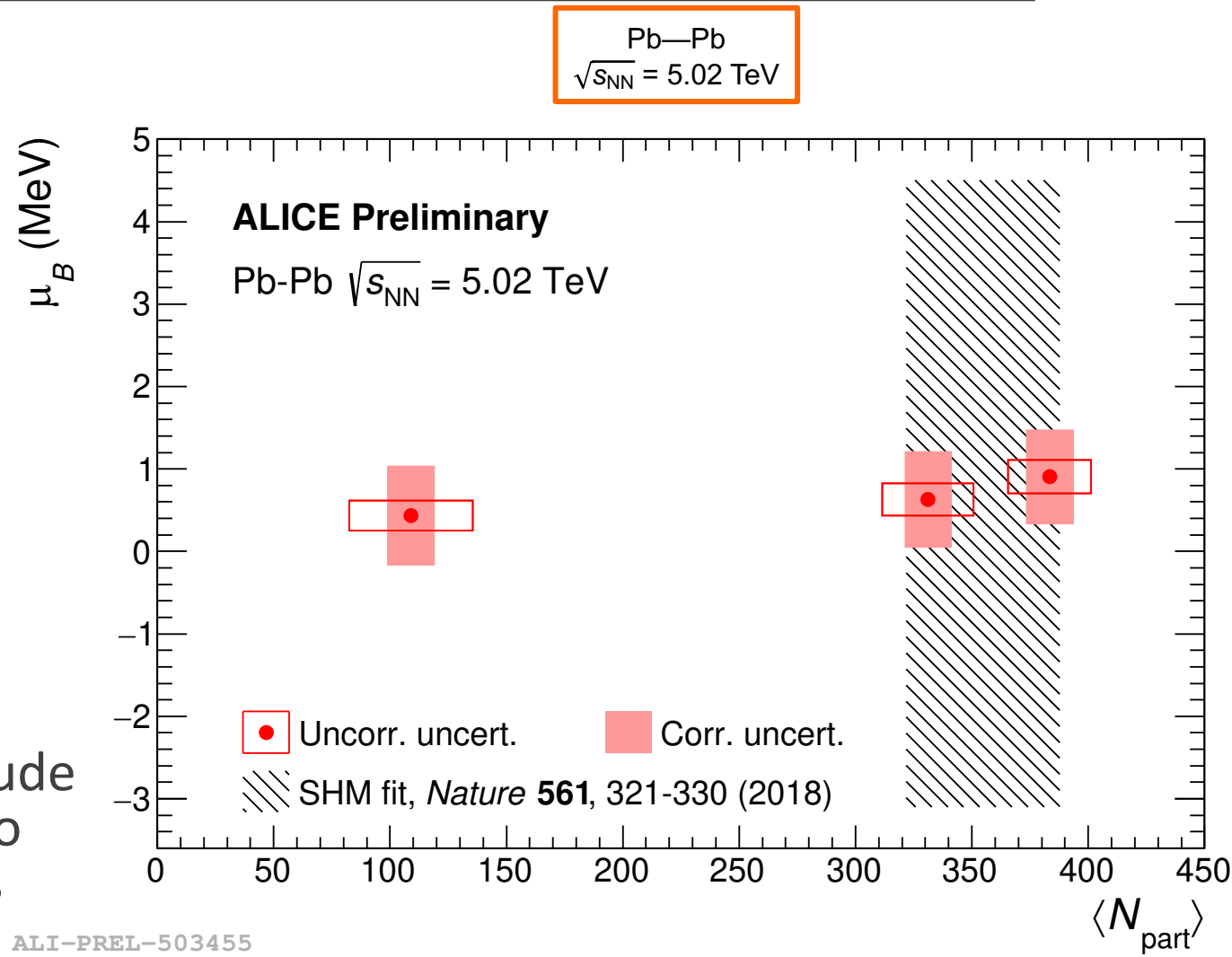
Hypertriton production

- Fit to the data provides a value of μ_B close to zero in the most central collisions
- Antiparticle-to-particle ratio compared to SHM predictions at $T_{ch} = 155 \pm 2$ MeV and using the obtained μ_B
- Very precise result even with large uncertainties for the hypertriton and a small overestimation for the ${}^3\text{He}$



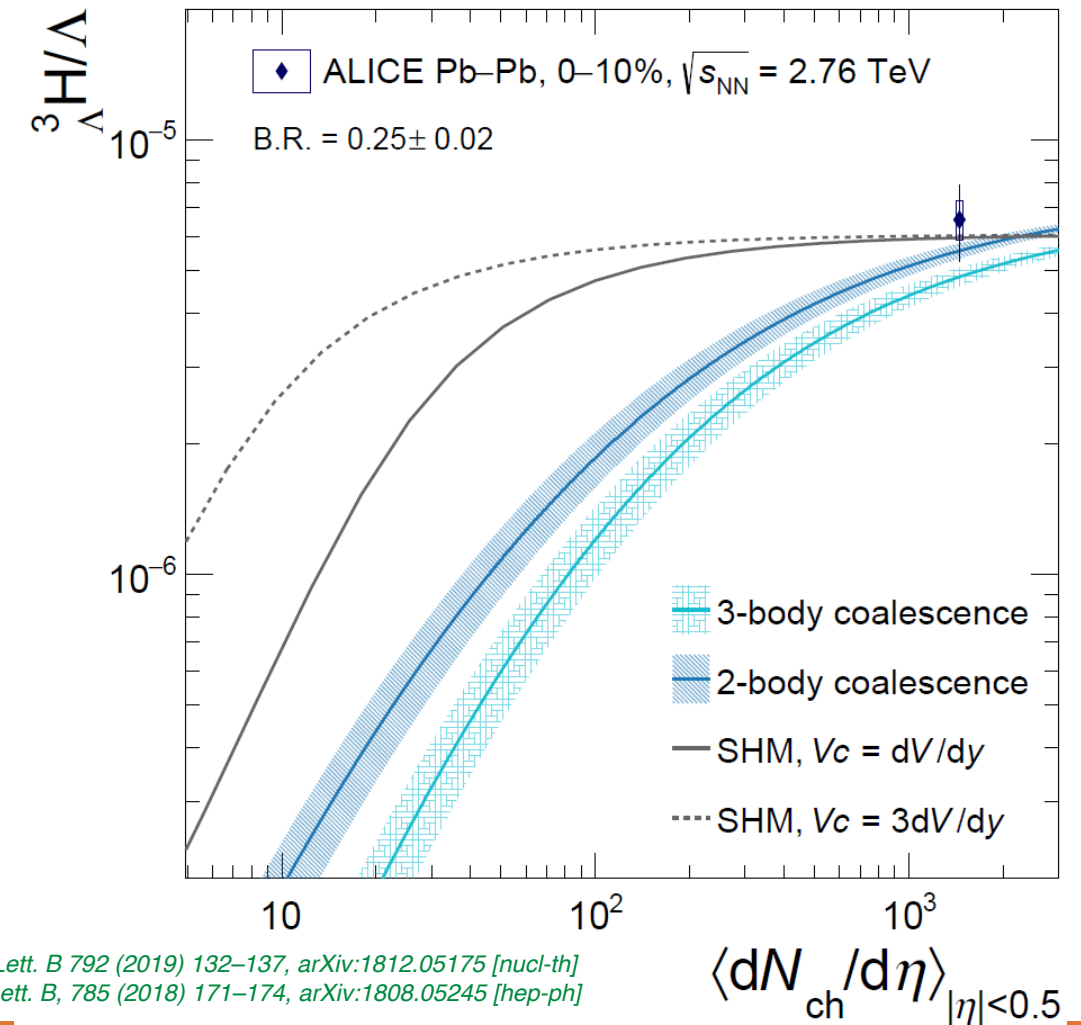
Hypertriton production

- Fit to the data provides a value of μ_B close to zero in the most central collisions
- Antiparticle-to-particle ratio compared to SHM predictions at $T_{ch} = 155 \pm 2$ MeV and using the obtained μ_B
- Very precise result even with large uncertainties for the hypertriton and a small overestimation for the ^3He
- Measurement of μ_B in different centralities nearly one order of magnitude more precise than the SHM fit thanks to cancellation of correlated uncertainties



Hypertriton production vs. multiplicity

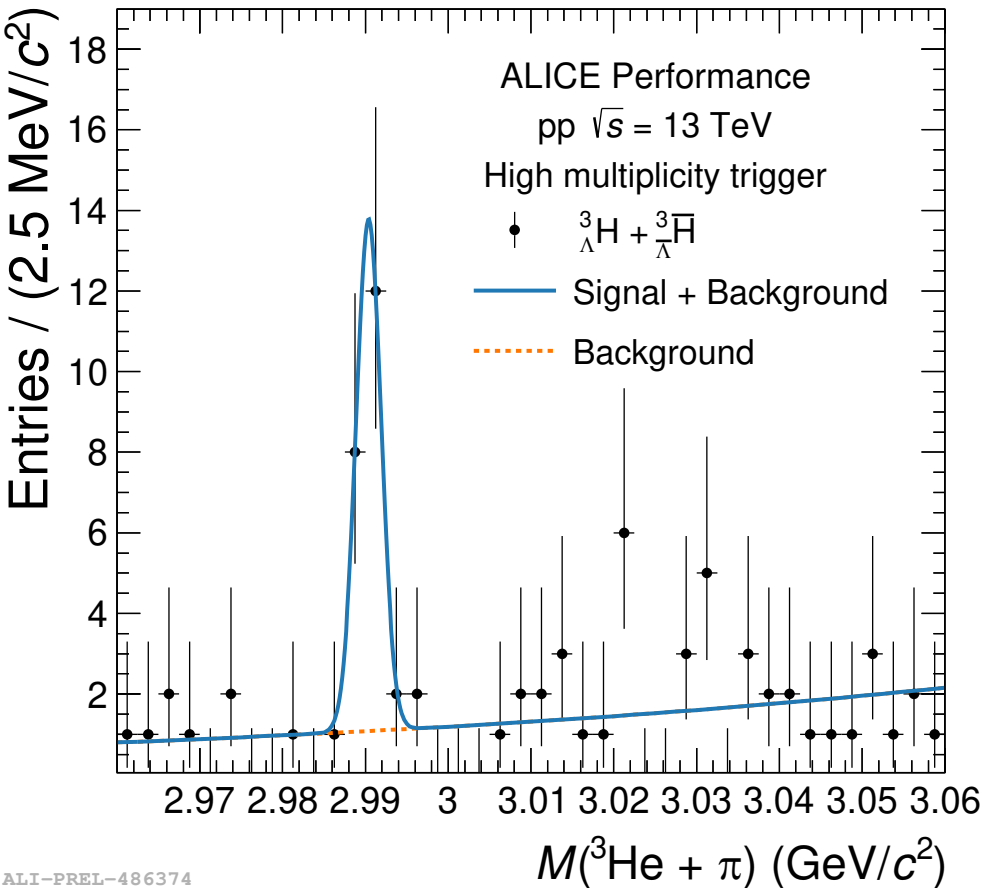
- ${}^3\Lambda/\Lambda$ ratio vs. multiplicity
- Perfect candidate to distinguish between coalescence and statistical hadronization models
- Extremely sensitive to the nuclei production mechanism:
 - For statistical hadronization models (SHM) the object size is not relevant
 - In a coalescence picture large suppression of the production in small systems expected due to the object size



Coalescence: K.-J. Sun, C.-M. Ko and B. Dönigus, Phys. Lett. B 792 (2019) 132–137, arXiv:1812.05175 [nucl-th]
SHM: V. Vovchenko, B. Dönigus and H. Stoecker, Phys. Lett. B, 785 (2018) 171–174, arXiv:1808.05245 [hep-ph]

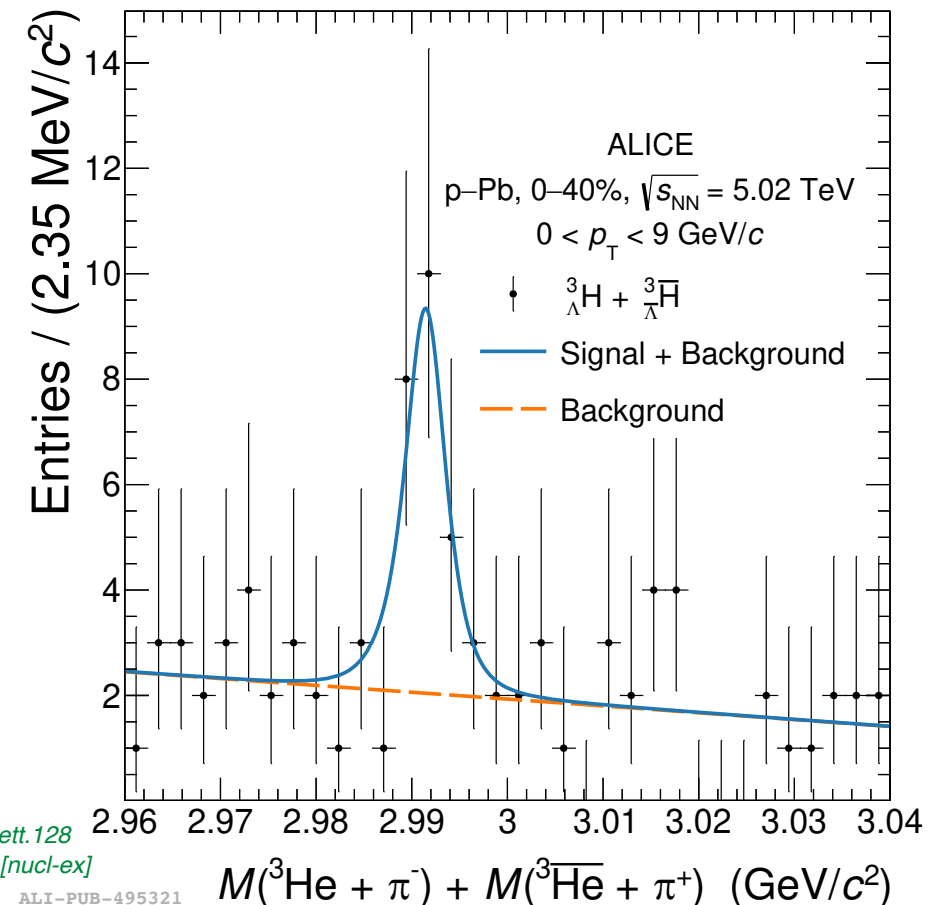
Hypertriton in small systems

pp



- First measurement of the hypertriton in pp (13 TeV) and p—Pb (5.02 TeV) collisions
- Signal extraction using topological and kinematic cuts (pp) or machine learning approach (p—Pb)

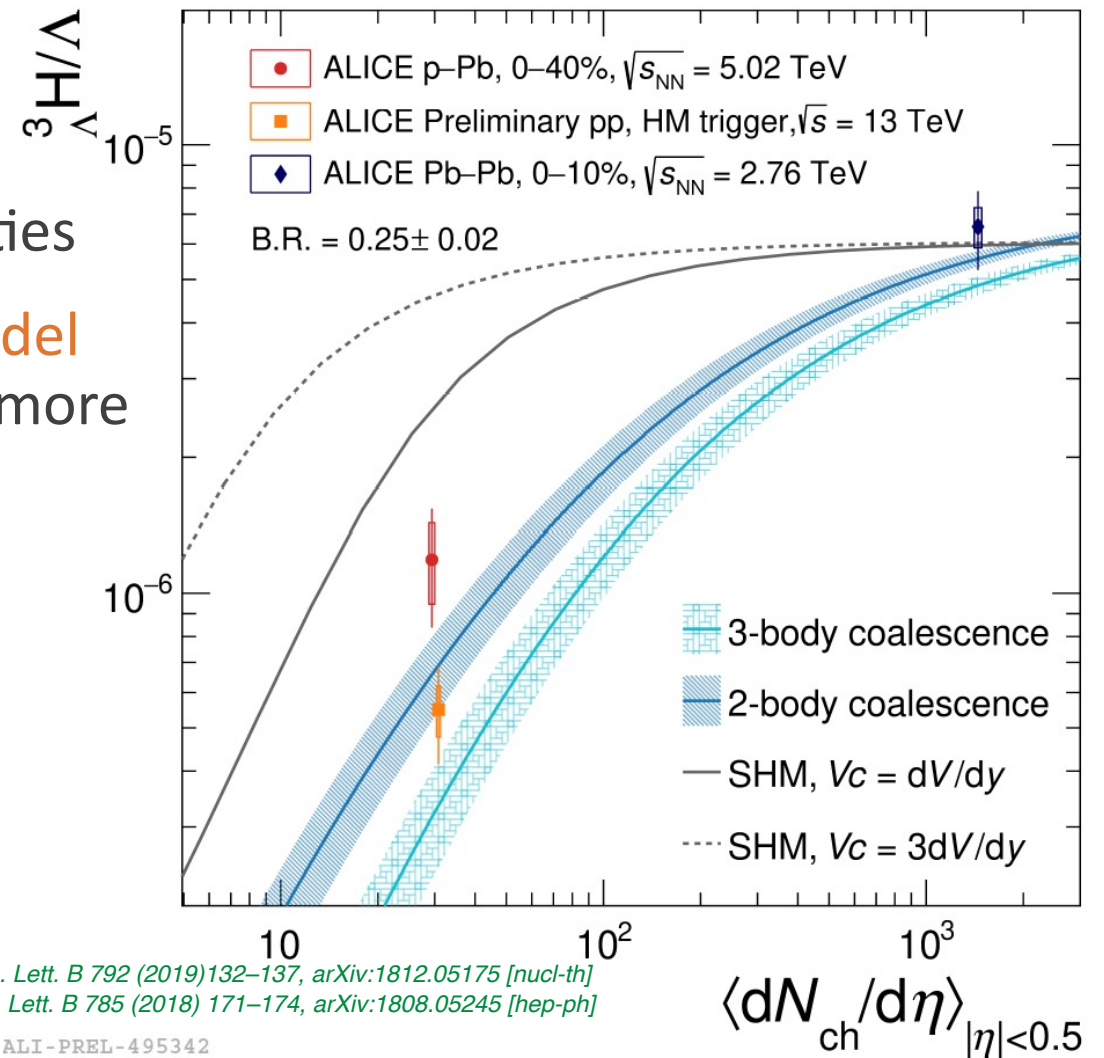
p—Pb



ALICE collaboration, Phys. Rev. Lett. 128 (2022) 252003, arXiv:2107.10627 [nucl-ex]

$^3\Lambda$ H / Λ ratio

- Measurements in pp and p–Pb:
Two new points at different multiplicities
- Leads to the exclusion of the **SHM model** implementation with $V_c = 3 dV/dy$ by more than 6σ
- Data slightly favours the **two-body coalescence**
- But does not exclude **three-body coalescence**

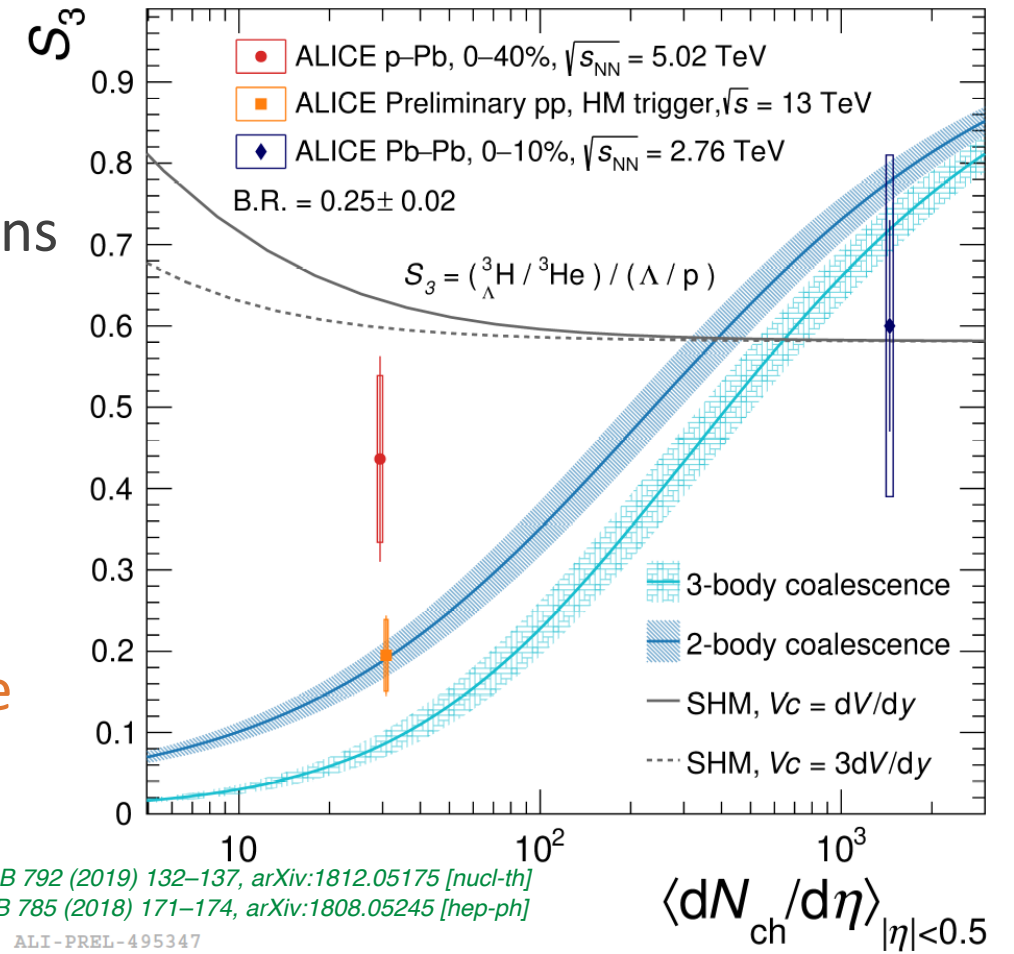


Coelescence: K.-J. Sun, C.-M. Ko and B. Döningus, Phys. Lett. B 792 (2019) 132–137, arXiv:1812.05175 [nucl-th]
SHM: V. Vovchenko, B. Döningus and H. Stoecker, Phys. Lett. B 785 (2018) 171–174, arXiv:1808.05245 [hep-ph]

ALI-PREL-495342

S_3

- $S_3 = (\Lambda / p) / ({}^3\text{He} / {}^3\text{H})$ vs. multiplicity
- Strangeness population factor for the measurement of baryon-strangeness correlations
- Penalty factor due to mass difference cancels and size effects can be studied
- Measurements in pp and p—Pb: two new points at different multiplicities
- Data slightly favours the **two-body coalescence**
- But does not exclude **three-body coalescence**



Coelescence: K.-J. Sun, C.-M. Ko and B. Dönigus, Phys. Lett. B 792 (2019) 132–137, arXiv:1812.05175 [nucl-th]
 SHM: V. Vovchenko, B. Dönigus and H. Stoecker, Phys. Lett. B 785 (2018) 171–174, arXiv:1808.05245 [hep-ph]

ALI-PREL-495347

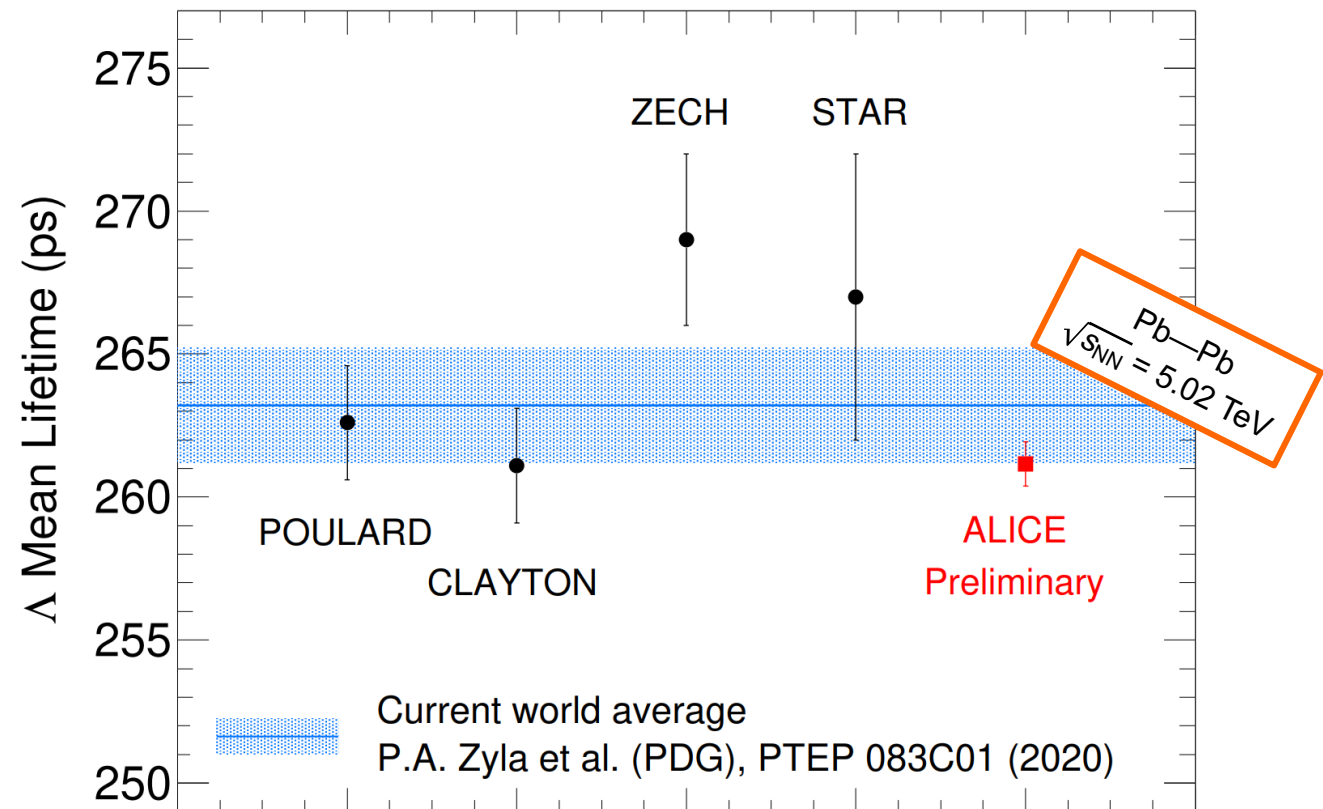
Summary

- ALICE is the ideal experiment to study the production and properties of light (anti)(hyper)nuclei in all collision systems
- The latest results, even though more precise than previous data, still do not allow for a strong conclusion about the dominant production mechanism
- The presented experimental results on mass and binding energy of the hypertriton support its loosely-bound structure
- The upcoming Run 3 and Run 4 will add more statistics for the measurement of light (anti)(hyper)nuclei
- This may also give the possibility of a more conclusive answer to the question of the production mechanism

Backup

Free Λ lifetime

- New, extremely precise measurement of the free Λ lifetime as reference for the hypertriton lifetime
- About a factor 3 more precise than the PDG value



ALI-PREL-505548